IS-1012

IOWA STATE UNIVERSITY

TRANSIT TIMES AND ELECTRICAL DISCHARGE IN A STEADY-STATE GAS ACTIVATION SYSTEM

by

David Thomas and Willard L. Talbert

AMES LABORATORY

RESEARCH AND DEVELOPMENT REPORT

U.S.A.E.C.

IS-1012

Physics(UC-34)
TID 4500, December 1, 1964

TRANSIT TIMES AND ELECTRICAL DISCHARGE IN A STEADY-STATE GAS ACTIVATION SYSTEM

by

David Thomas and Willard L. Talbert

November, 1964

Ames Laboratory

at

Iowa State University of Science and Technology
F. H. Spedding, Director
Contract W-7405 eng-82

This report is distributed according to the category Physics(UC-34) as listed in TID-4500, December 1, 1964.

Printed in USA. Price $ 3.00. Available from the Clearinghouse for Federal Scientific and Technical Information, National Bureau of Standards, U. S. Department of Commerce, Springfield, Virginia

TABLE OF CONTENTS

IS-1012

IS-1012

TRANSIT TIMES AND ELECTRICAL DISCHARGE IN A STEADY-STATE GAS ACTIVATION SYSTEM*

David Thomas and Willard L. Talbert

ABSTRACT

This study deals with the problem of transporting a gas from the core of the Ames Laboratory Research Reactor to the ion source of an electromagnetic isotope separator in a steady-state fashion. The parameters on which this flow depends are ascertained so that the flow may be predictably controlled by a computer. The transit time through the activation line is calculated and confirmed experimentally for nitrogen and xenon. The initiation of an electrical discharge in the low pressure gas by a 60 kv potential is studied as a function of the gas and the gradient length.

---

*This report is based on a Master of Science thesis submitted by David Thomas November, 1964, to Iowa State University, Ames, Iowa.

I. INTRODUCTION

A. Isotope Separator System

A system is now being constructed at the Ames Laboratory Research Reactor for detailed analysis of the nuclear decay of short-lived radioisotopes. This system will be described to give the context in which the present study is placed.

It is desired to accumulate much more high resolution data on the beta decay spectra of radioisotopes throughout the Chart of Nuclides with half-lives down to a few seconds. Of special interest are the rare-earth elements from atomic number 58 through 71. A study of the Chart of Nuclides has shown that there are 160 beta decaying nuclei with half-lives between one and 180 seconds which are producible by neutron irradiation of a stable or long-lived parent. To date, few of these have been studied with high resolution beta spectrometers because of the relatively long time required for these measurements and the very special requirements for a spectrometer source. Such a source must have the radioactive atoms in a very thin layer at the surface, so the emitted beta particles do not have their energy significantly degraded while emerging from the source. This requirement becomes more stringent as one strives for higher

resolution of the momenta. Presently, to make such a source with high specific activity, the activated atoms must be chemically or physically separated from the unactivated and then deposited in a thin film on the source foil. This lengthy process prohibits the careful study of short-lived beta activities.

The system which is being built at the Ames Laboratory Research Reactor to provide the capability of analyzing short-lived beta activities is shown in Figure 1. The nuclide to be studied will be one which is obtainable by (n,γ), (n,α) or (n,d) reaction or by fission using a stable or long-lived parent. The products of all of these reactions differ in mass from the parent; thus they can be separated electromagnetically. A solid sample containing the isotope from which the desired nuclide will be produced will be placed in the neutron flux in the core of the reactor at the end of a tube one half to one inch in diameter and about twelve feet long. This tube will transport the molecules to the separator ion source. Heating elements will surround this tube making it possible to raise its temperature to 700 to 1000^{o} C and vaporize the sample at a controlled rate. With the sample constantly in the flux it will be assured that the vaporized molecules will always be at saturated activity. The ratio of activated to unactivated atoms at saturation is given by

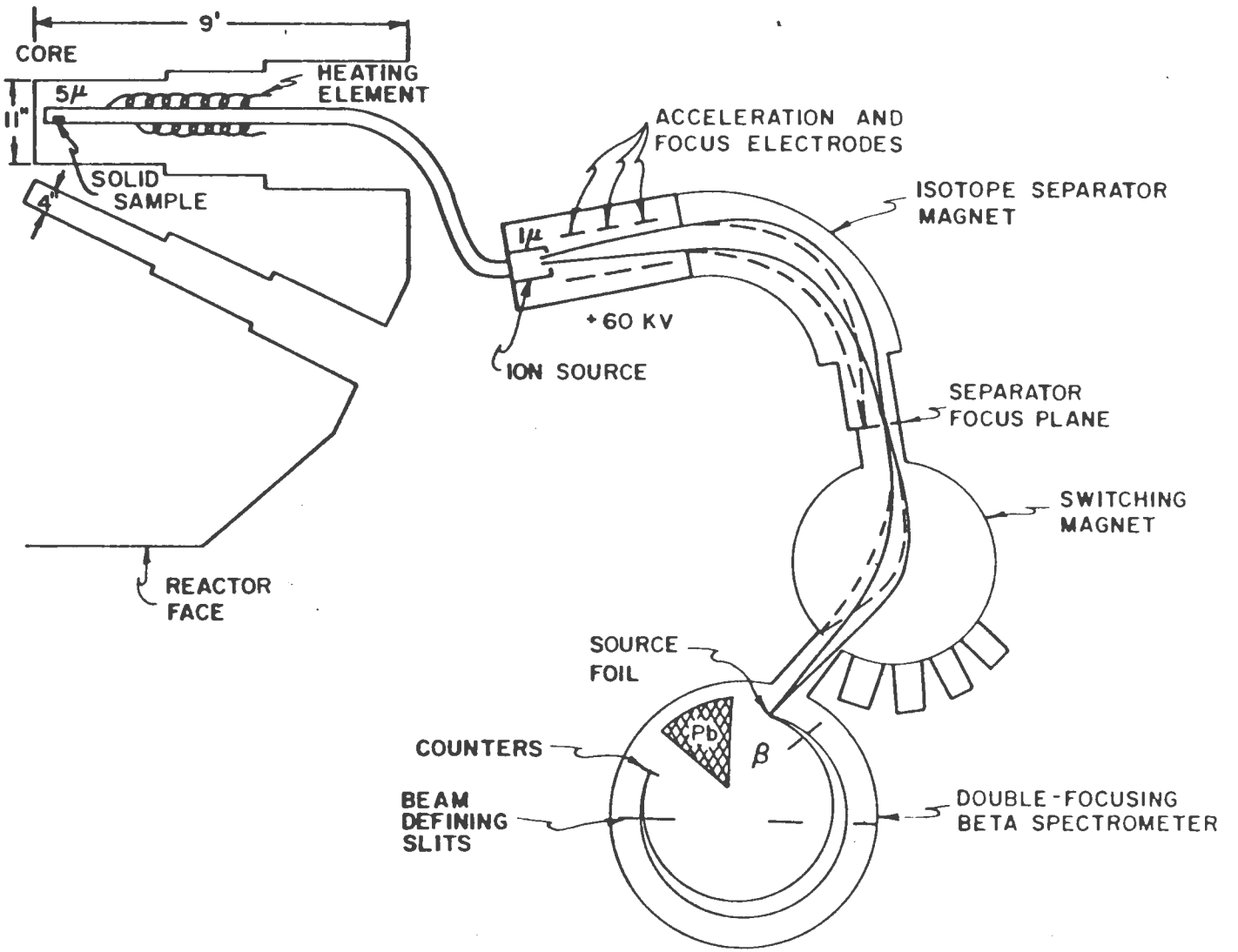

Figure 1. System for rapid analysis of beta activities produced in the Ames Laboratory Research Reactor.

$$\left.\frac{B}{A}\right|_{sat} = \frac{\sigma\varphi}{\lambda_B - \sigma\varphi} \qquad 1$$

where σ is the pile neutron cross section for the desired nuclear reaction, φ is the thermal neutron flux, and λ_B is the decay constant for the reaction product. This ratio typically will be 10^{-6} to 10^{-8}, indicating that a very high degree of isotope separation will be necessary to provide a nearly pure source.

The electromagnetic isotope separator, which was built in Stockholm, Sweden, was purchased from NUCLESA of Geneva, Switzerland, and will provide a total ion current of about one hundred microamps at an accelerating potential up to seventy kilovolts. Then, even if $\frac{B}{A} = 10^{-8}$, the current of radioactive atoms will be 6×10^6 ions per second. As shown in Figure 1 all current beams of mass other than the desired radioactive one will be stopped, and only it will be allowed to proceed through the switching magnet to be deposited at the source position of a high resolution double-focusing beta spectrometer. The switching magnet will be included in the system to permit the directing of the beam to other experimental arrangements and also to provide a second stage of isotope separation. Thus, this scheme will render a ready-to-be-analyzed beta source with the following properties:

1. Little of the source activity will have been lost,

because the transit time from the reactor to the ion source of the isotope separator is only a few seconds, and the transit time through the separator and switching magnet is a negligible fraction of the half-life.

2. The source will be isotopically pure and therefore free from contaminating nuclear radiations from nuclei of different mass and from parent nuclei which can mask the active nuclei and degrade the radiation.

3. Since the depositing beam consists of heavy ions with energies between 40 and 70 keV, these ions will not penetrate deeply into the source foil meeting this requirement for a good beta source.

4. The source activity as a function of time is given by

$$\lambda_B B = I_B[1 - e^{\lambda_B t}] \qquad 2$$

where I_B is the number of radioactive atoms deposited per second. Of course, at t = 0, when the beam is turned on, the activity is zero. It builds up with time as the exponential term becomes small. After a few half lives the activity will just be equal to the current and will remain so. If a steady current can be maintained, there will be effectively

an infinitely long-lived source on which very careful, statistically improved beta spectroscopy can be accomplished.

To keep this current, and therefore the activity, constant it is planned to employ the real-time computing system which will be available at the reactor. The problems which are presented in parts B and C are directly involved with the real-time control of this system. The problem of part D is one that must be answered prior to the design of the transport line.

B. Gas Flow Problem

The ion source of the isotope separator, Figure 2, is a cylindrical discharge chamber about 50 mm long and 20 mm in diameter surrounded by a coil producing a magnetic field along the axis. Near the gas inlet is a hot filament to provide electrons. The wall of the cylinder, or anode, is kept slightly positive with respect to the ends. The electrons oscillate between the ends, traveling in spiral paths due to the magnetic field and the attraction by the anode. This is known as the Nielsen source (1; 2, p. 53).

The ion current delivered by the source and the resolving power, which is also an important parameter of a separation, depend upon the dimensions of the source, the anode potential, the magnet current, the accelerating, extraction

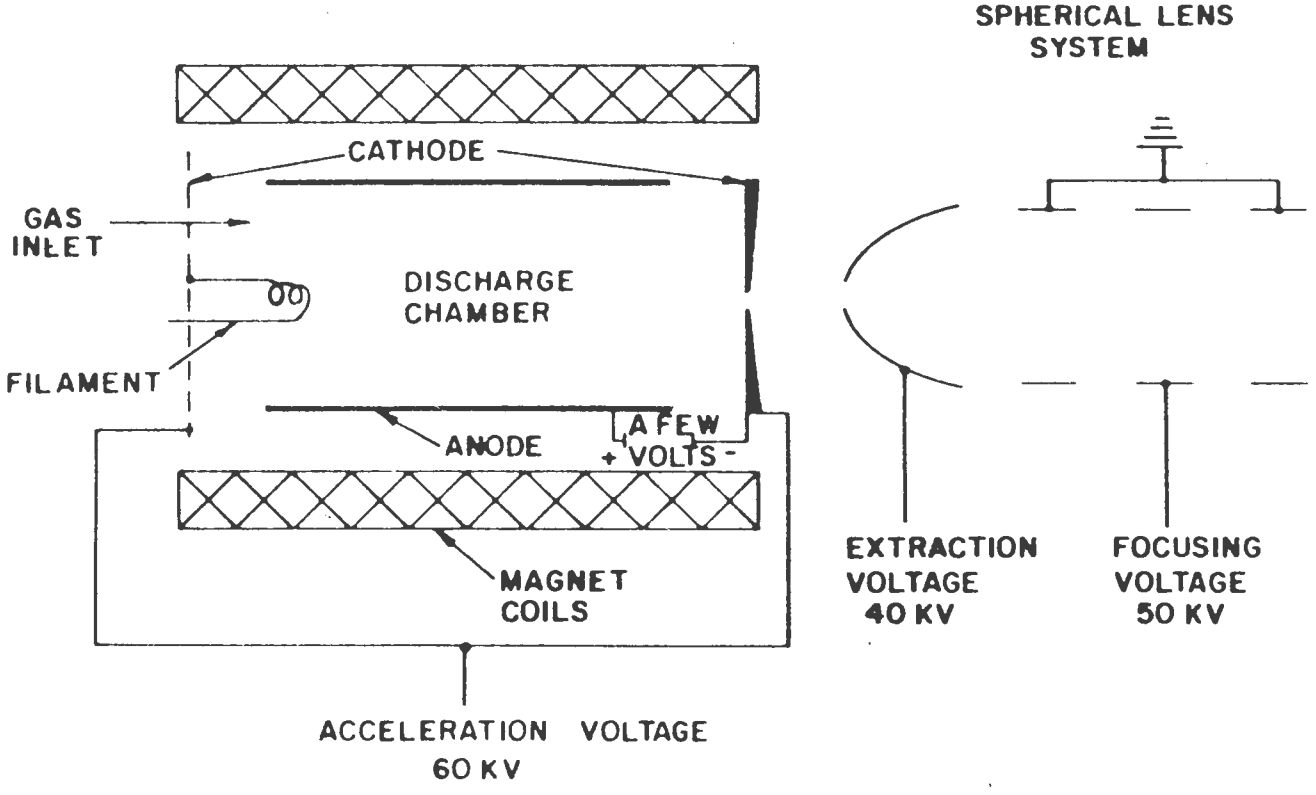

Figure 2. Schematic of ion source and extraction and focusing systems of the isotope separator.

and focusing voltages, the pressure in the discharge chamber and the filament current (3). Of these parameters the most useful for control of the ion current are the accelerating voltage and the filament current. When the ion current is varied by adjusting the filament current, the resolving power can be returned to maximum by adjusting the focusing voltage.

The dependence of the maximum separator ion current and resolving power on discharge chamber pressure is shown in Figure 3 (1; 2, pp. 270-274). Below P_{min} the discharge fails completely. P_{min} depends on the ionization cross section of the gas used and the geometry of the source. For the Nielsen source it is about 2 to 4 x 10^{-4} mm Hg. Above 1.5 x 10^{-3} mm the ionization efficiency decreases sharply resulting in a decreasing ion current. The resolving power also decreases as a result of the increased pressure in the acceleration chamber causing more scattering of the beam. Thus it will be necessary during a separation to maintain the discharge chamber pressure within these limits.

A study is herein made of the gas flow characteristics in a tube simulating the transport line which will carry the activated gas from the reactor core to the ion source. The parameters which govern the sample pressure necessary to maintain the discharge chamber pressure in the required range are determined. This pressure then establishes the temperature at which the sample must be kept and also the tempera-

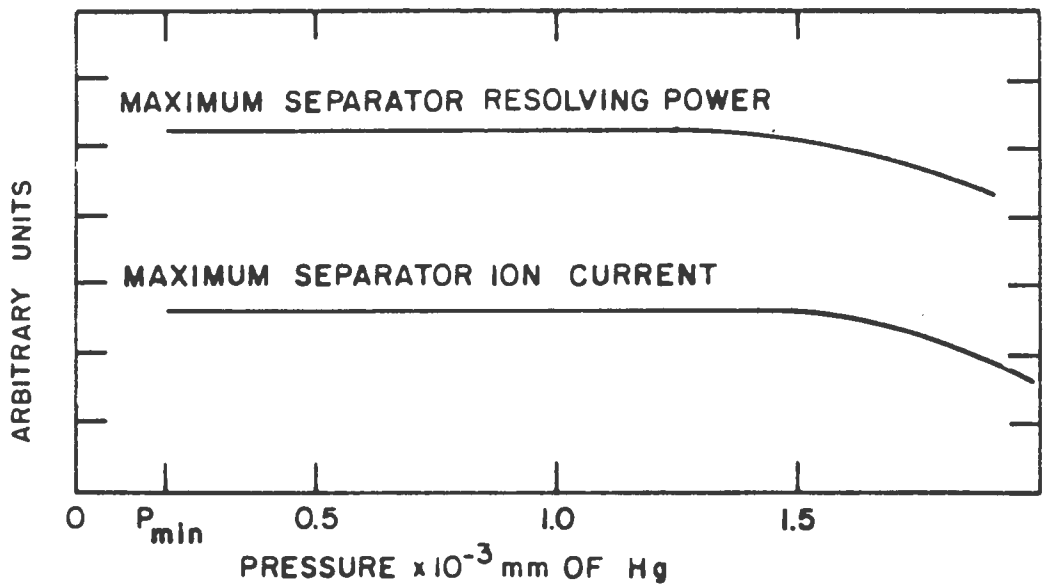

Figure 3. Maximum separator ion current and resolving power in arbitrary units as a function of pressure in the discharge chamber

ture of the transport line necessary to prevent condensation.

C. Transit Time

It is necessary to know the transit time of molecules from the sample in the reactor core to the ion source. This time determines the lower limit of half-lives which may be studied. However, activities with half-lives considerably less than the transit time can be studied if their activation cross sections are great enough to leave sufficient activity after having decayed for the duration of the transit, or if the corresponding decrease in statistical precision due to the loss of counts is acceptable.

Although the operating pressure is not critical as long as it is within the stated limits, it still must be possible to control this pressure to keep it within the limits. The time required to make a pressure correction by controlling the temperature of the sample in the reactor depends on the transit time. In this study the transit times are calculated and then experimentally confirmed for the pertinent pressure range.

D. Electrical Discharge Problem

The last matter of concern in this study arises from the dilemma that the ion source must be at the high, positive accelerating potential, nominally 60 kV, and the activation

line leading into the reactor preferably should be grounded. It is conceivable that the entire line could be electrically insulated allowing it to be at 60 kV all the way into the reactor. This, however, would cause serious practical difficulties. Then, somewhere between the ion source and the reactor face, an insulating section of tubing must be inserted establishing a 60 kV gradient. On the outside of the tube there is no problem, since it can be electrically insulated to prevent discharge. On the inside, however, the electric field exists in rarified gas resulting in favorable conditions for a gas discharge. Such a discharge cannot be tolerated, because of the resulting disturbance to the flow of gas to the ion source. Furthermore, a discharge would create a short across the insulating section and ground the accelerating potential on the ion source. This clearly would be disastrous to the efforts to maintain a steady ion current.

A large amount of work has been done in the past on electrical sparking and discharge. However, Paschen's Law, which is the guidepost of most gas discharge work, does not cover the range of pressures or potentials with which the present problem is concerned (4, 5, 6). Nor has any of the previous work been done with this particular geometrical configuration. Instead most of it has been for the case of parallel plate electrodes. So it was decided to conduct studies on the particular gas discharge problem presented by

the described system.

Extrapolation from available information indicates that if the 60 kV potential could be applied over a very short distance, establishing a large potential gradient, it might be possible to avoid a discharge. The initiation of a discharge requires that charged particles accelerated in the electric field must make a sufficient number of collisions with gas particles to create an avalanche of ionizing events. If the field is constrained to act over a length of the order of one mean free path of the gas molecules at that pressure, it seems reasonable that a discharge could not be sustained. This contention has been tested as a function of gap length, mean free path and voltage.

II. GAS FLOW

A. Theoretical Study

As pointed out in section I.B. the pressure at the ion source must be between 2×10^{-4} and 1.5×10^{-3} mm Hg. It is important to know what the pressure at the sample end of the transport line must be to fulfill this requirement. The kinetic theory of gases may be applied to the system to calculate this pressure gradient. The system will be treated simply as a long tube which is pumped out through a small aperture at one end as shown in Figure 4. It is possible to employ a screen-like back on the discharge chamber as indicated in Figure 2. It would not impede the gas flow, which is determined by the pumping speed of the exit aperture.

The well-known result from kinetic theory for the number of molecules striking a unit surface area in unit time is (7, pp. 21-22)

$$N = \frac{n\bar{v}}{4} \qquad 3$$

where n is the number of molecules per unit volume and $\bar{v}$ is the mean speed of the molecules as defined by

$$\bar{v} = \int_0^\infty v f(v) dv \ . \qquad 4$$

Here f(v) is the Maxwell-Boltzmann distribution function for the molecular velocities. It is easily shown that the mean speed is given by (7, p. 78)

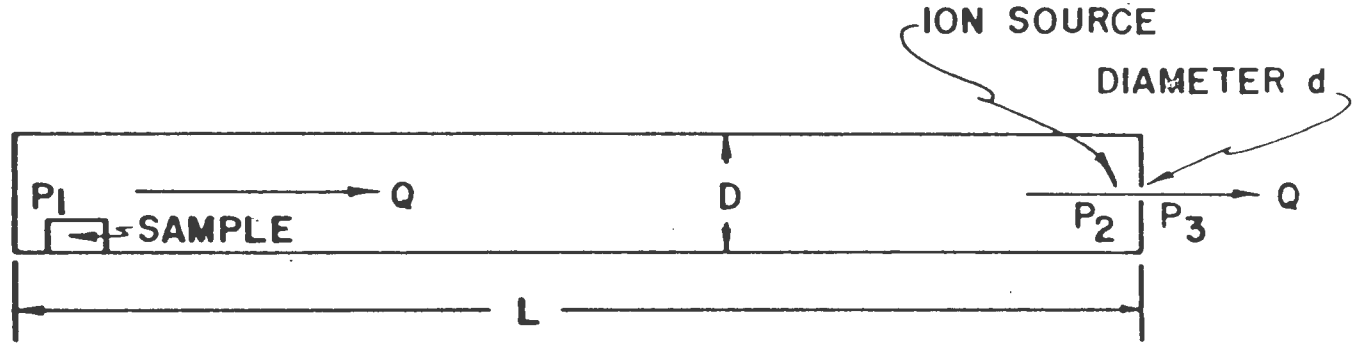

Figure 4. Schematic of transport line terminating in the ion source

$$\bar{v} = \left[\frac{8kT}{\pi m}\right]^{\frac{1}{2}} . \qquad 5$$

Then the number in unit time going through a very thin-walled hole of area A, diameter d, is $\frac{An\bar{v}}{4}$. A thin wall is specified so that the edge effects for a molecule approaching the hole at nearly right angles to its axis are unimportant. One is justified in simply multiplying the flux of molecules by the area only if the molecules proceed through the hole independently of each other. This requires that there be essentially no collisions in the vicinity of the hole. The mean free path of molecules at pressure P and temperature T is given by (7, p. 32)

$$\lambda = \frac{kT}{\sqrt{2}\pi P\sigma^2} \qquad 6$$

where σ is the molecular diameter. At room temperature and a pressure of 1 micron λ is 4.8 cm for nitrogen and 2.8 cm for xenon. Since the exit aperture of the ion source is nominally 1.5 mm, this approach is justified.

The phenomenon discussed here is called effusion. It clearly applies through the hole in both directions, so the net flow is proportional to the difference in molecular densities on the two sides. Here the reverse flow may be neglected, because the isotope separator utilizes a differential pumping system which places a large diffusion pump near the exit aperture to keep the pressure low--roughly one

per cent of that in the source.

From the perfect gas law

$$P = nkT, \tag{7}$$

which clearly applies for this low pressure gas, and equation 5, the final result is

$$Q = \frac{AP_2}{[2\pi mkT]^{\frac{1}{2}}} \tag{8}$$

where Q is the number of molecules effusing through the exit aperture in unit time and P_2 is the ion source pressure.

In this study it will be assumed that Q, as calculated above, represents the total flow of gas through the ion source of the isotope separator. In reality there is another component to the flow; this, of course, being the ion current. The current is extracted by means of electric fields and therefore does not depend on P_2 (except to the extent that the plasma density depends on P_2). However, the efficiency of the source is quite low; usually just a few per cent at maximum. Thus, in assuming that the gas flow through the source consists entirely of neutral molecules obeying kinetic theory, the error is small. This same assumption is made by Koch (2, p. 271) in the calculation of ion source performance.

Next an expression for the flow Q in the tube as a function of the pressure gradient will be derived. From molecular transport theory Fick's Law for the net number of molecules transported across a unit area per unit time

$$\frac{Q}{A} = -\frac{1}{3} \bar{v} \lambda \left.\frac{dn}{dx}\right|_{x=0} \qquad 9$$

may be derived (7, p. 60). Here the derivative is evaluated at the plane across which the flux is desired. The proportionality between the flux and gradient of particles

$$\frac{Q}{A} \equiv -\mathcal{D} \left.\frac{dn}{dx}\right|_{x=0} \qquad 10$$

defines the diffusion coefficient, so

$$\mathcal{D} = \frac{1}{3} \bar{v} \lambda \ . \qquad 11$$

If the gas pressure in the transport line is so low that $\lambda >> D$, the condition is met for so-called free-molecule or molecular flow. Under this condition most collisions of the gas molecules are with the tube wall rather than with other molecules. These collisions have been shown to be "diffuse" rather than "specular" (7, p. 56). This means that a molecule's direction upon leaving the wall after a collision bears no relation to its incident direction, and the problem may be treated as one of random diffusion. This is due to the irregularity of the surface on a microscopic scale and the fact that the molecules may adhere to the surface for a finite length of time.

In molecular flow the average distance traveled by a molecule between two wall collisions equals the tube diameter (7, p. 70). Thus let $\lambda \rightarrow D$ in equation 9 giving

$$Q = \frac{-\pi D^3}{12} \bar{v} \frac{dn}{dx} \ . \qquad 12$$

The pressure gradient is linear, so

$$\frac{dn}{dx} = - \left[\frac{n(1) - n(2)}{L}\right] . \qquad 13$$

Again invoking relations 5 and 7 the result is

$$Q = \frac{\pi D^3}{12} \left[\frac{8}{m\pi kT}\right]^{\frac{1}{2}} \frac{\Delta P}{L} \qquad 14$$

where ΔP is the pressure gradient over the length of the tube.

For the steady-state molecular flow, expressions 8 and 14 for Q may be equated giving

$$\Delta P = \frac{0.75\ L\ d^2}{D^3} P_2 . \qquad 15$$

Interestingly enough, ΔP is determined purely geometrically and is independent of the nature of the gas and the temperature as long as the flow is molecular in nature.

Results will be stated in terms of the ratio of P_1 to P_2, where

$$P_1 = P_2 + \Delta P. \qquad 16$$

In the experimental arrangement, which is described in the next section, the length L between discharge gauges was 363 cm, and the diameter D was 1.27 cm. Putting these constants into equation 15 gives from equation 16

$$\frac{P_1}{P_2} = 1 + 1.33\ d^2 \qquad 17$$

where d is the aperture diameter in millimeters. For d = 1.5 mm and an ion source pressure of one micron, P_1 is four microns. At this pressure for both nitrogen and xenon, which were the

gases investigated, the condition $\lambda \gg D$ is not fulfilled. However, it is suspected that, even though the criterion for molecular flow is not strictly satisfied, the flow will still be predominately molecular, because a gas does not become significantly viscous until at much higher pressures than are encountered here.

An empirical relation first given by Knudsen (8, p. 27) describes the conductance of a long cylindrical tube over the entire range of molecular through viscous flow. It is given by

$$C = \frac{\pi D^4 \bar{P}}{128 \eta L} + \left[\frac{1}{6}\left(\frac{2\pi kT}{m}\right)^{\frac{1}{2}} \frac{D^3}{L}\right]\left[\frac{1 + \left[\frac{m}{kT}\right]^{\frac{1}{2}} \frac{D\bar{P}}{\eta}}{1 + 1.24\left[\frac{m}{kT}\right]^{\frac{1}{2}} \frac{D\bar{P}}{\eta}}\right] \qquad 18$$

in cgs units, where η is the viscosity of the gas, and

$$\bar{P} = \frac{P_1 + P_2}{2} . \qquad 19$$

Conductance is defined by

$$C \equiv \frac{Q}{\Delta P}$$

which gives for the molecular conductance of the tube from equation 14

$$C = \frac{\pi D^3}{12L}\left[\frac{8}{m\pi kT}\right]^{\frac{1}{2}} \qquad 20$$

in $\frac{\text{molecules - cm}^2}{\text{sec-dynes}}$.

Two useful conversion factors are

$$1 \frac{\text{molecule}}{\text{sec}} = kT \frac{\text{dynes - cm}^3}{\text{cm}^2 \text{ - sec}} \qquad 21$$

$$1 \text{ micron} = 1.32 \frac{\text{dynes}}{\text{cm}^2} . \qquad 22$$

Converting equation 20 by means of 21 to the more meaningful units for conductance of cc per second gives

$$C = \frac{1}{6} \left[\frac{2\pi kT}{m}\right]^{\frac{1}{2}} \frac{D^3}{L} . \qquad 23$$

This is seen to be identical to the first factor of the second term in equation 18. The first term is the expression for the viscous conductance of a tube (8, p. 27). When $\overline{P}$ is very small the viscous term is negligible. When $\overline{P}$ is very large the first term becomes large with respect to the second, and predominately viscous conductance results.

A plot of the conductance from equation 18 for the transport tube for nitrogen and xenon at room temperature is shown in Figure 5. The highest $\overline{P}$ which will be encountered in the transport line is about four microns. This curve shows no effect at this pressure due to viscous flow for nitrogen. For xenon, however, at this pressure there appears to be a noticeable effect.

In the measurements which follow, the pressures at the two ends of the transport tube are recorded under equilibrium flow conditions of nitrogen and xenon. These are studied to

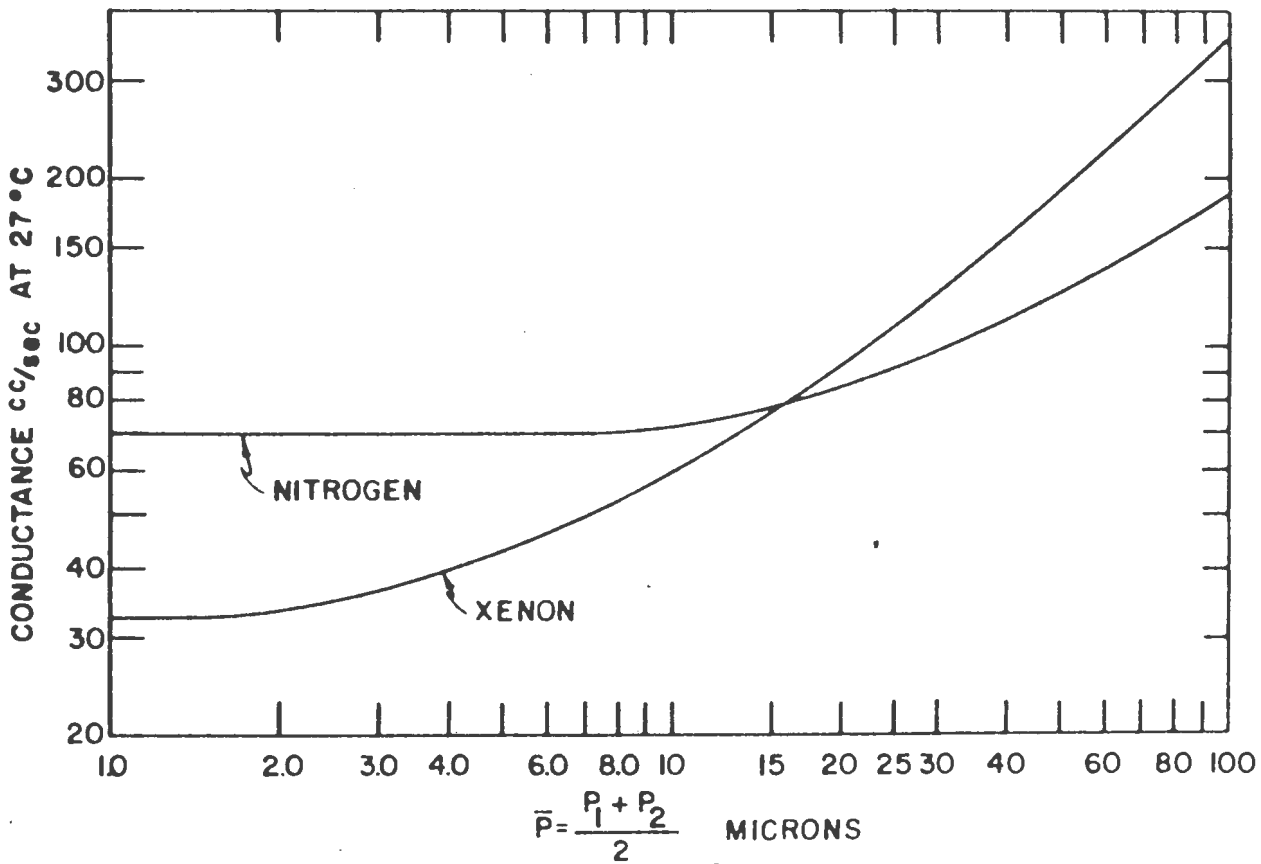

Figure 5. Conductance of the transport line at 27°C for nitrogen and xenon

see if the flow characteristics can really be treated as predominately molecular in nature, with perhaps a small correction for viscous flow, even though the strict criterion for molecular flow is not satisfied.

B. Experimental Investigation

1. Experimental arrangement

A vacuum system was built to simulate the transport line-ion source arrangement. It is illustrated in Figure 6. The pressures P_1 and P_2, at the reactor end and the ion source end respectively, were measured by means of cold cathode discharge gauges. A variable leak, with which the flow of gas was controlled, was placed at the reactor end. Provisions were made for changing the exit aperture to allow a check of the dependence of ΔP on d. The figure shows a detail of this arrangement. Immediately on the diffusion pump side of the aperture the volume per unit length was increased 16-fold. This, combined with the high pumping speed of the diffusion pump (100 liters per second) relative to that of the aperture, insured that the pressure on this side was negligible. The pressure at this point was monitored with a Veeco thermionic ionization gauge and was found to always be at least two orders of magnitude less than P_2.

The diffusion pump was a two-inch fractionating pump manufactured by Consolidated Vacuum Corporation. A new pump fluid,

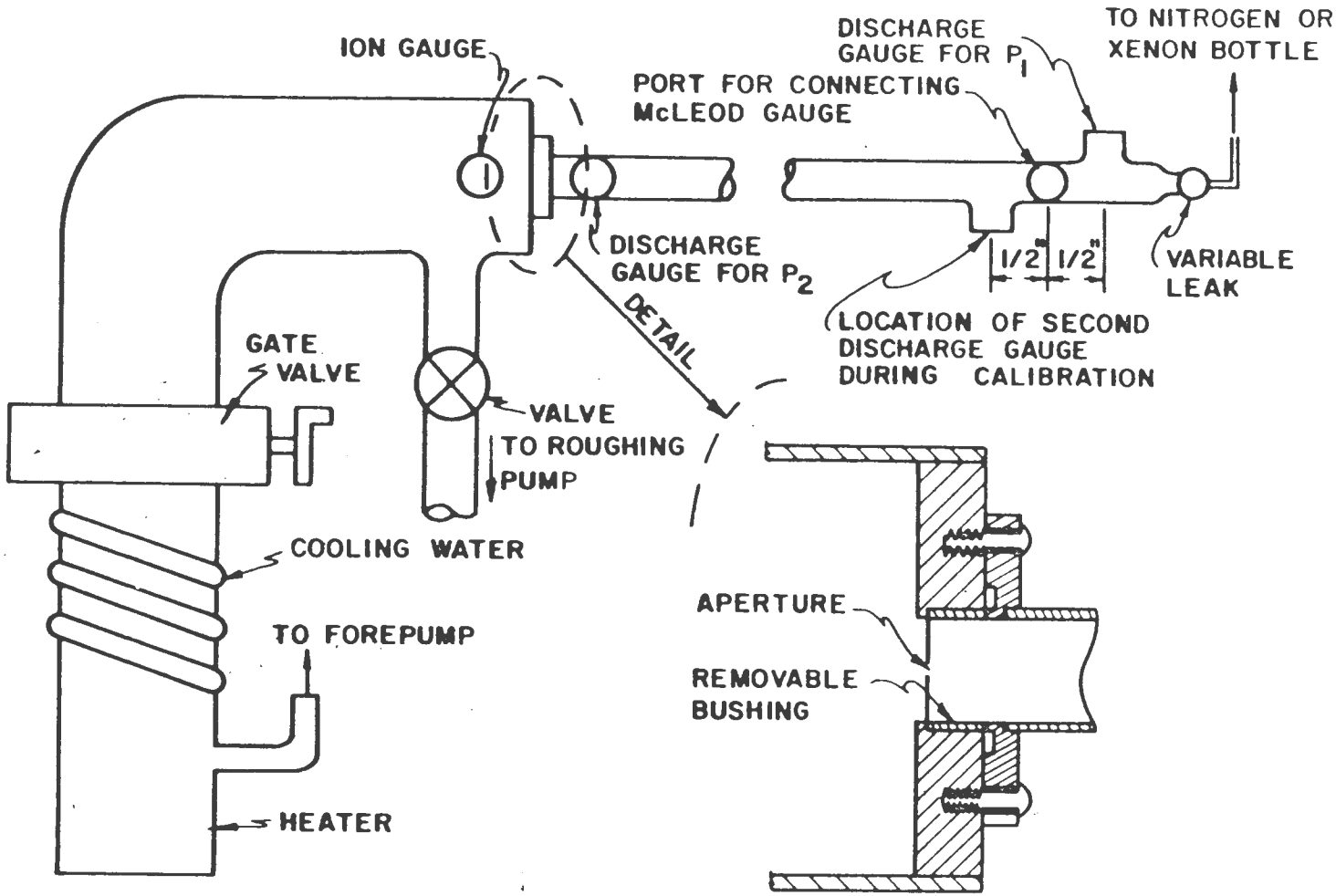

Figure 6. Schematic of the complete vacuum system showing locations of pressure gauges.

Convalex-10, which has very low vapor pressure, was used. This made it possible, without any baffle system and with the only cooling being the water on the pump, to reach an ultimate pressure at the ion gauge of 6×10^{-7} mm. This was obtained even when pumping through the smallest aperture. A two-inch gate valve surmounted the pump to permit venting the system independently from the pump.

2. Measurement of pressure

Calibration of the discharge gauges was done with a McLeod gauge, Figure 7, which measures pressure by direct application of Boyle's Law. This gauge was connected to the vacuum system at the port indicated in Figure 6. The gauge uses mercury which has a vapor pressure of about one micron at room temperature, so a dry ice cold trap was included between the gauge and the system. At the temperature of dry ice, $-78^{\circ}C$, the mercury vapor pressure is 3×10^{-9} mm. That the glass system was leak-free was verified by the fact that the same base pressure at the ion gauge was attained with or without the McLeod gauge being connected. The base pressure at the gauge itself was less than 0.01 micron, the lowest readable pressure on the gauge. The precision of the McLeod gauge is one per cent at ten microns, three per cent at one micron and ten per cent at 0.1 micron.

The discharge gauges were calibrated simultaneously by leaving the gauge for P_1 at its usual location, connecting the

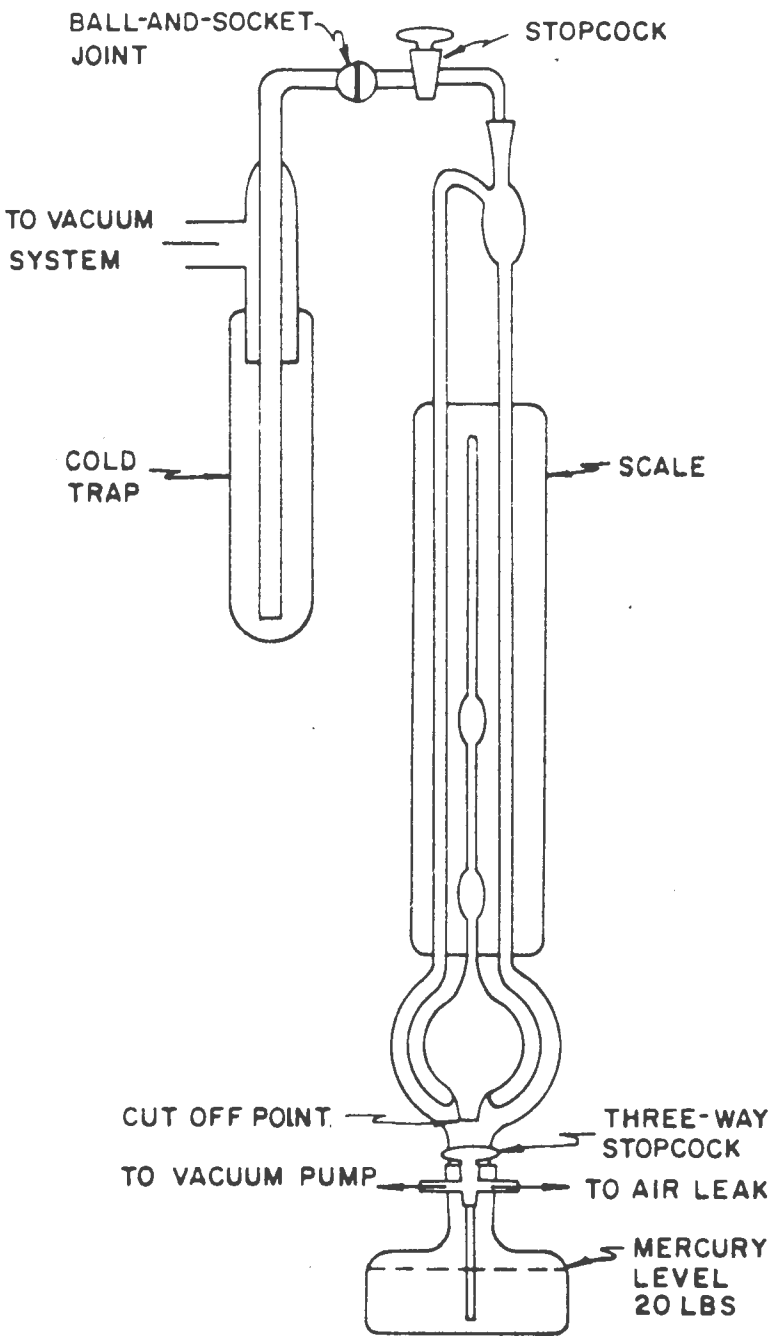

Figure 7. McLeod gauge with cold trap.

McLeod gauge at its port, and connecting the gauge for P_2 at the remaining port on the other side of the McLeod gauge as shown in Figure 6. The error introduced by the short tube length between the McLeod gauge and each of the discharge gauges was negligible. The variable leak proved to be a very sensitive and stable control of the pressure. Pressure readings with the McLeod gauge were highly reproducible.

The discharge gauges operate by placing a high positive potential on a wire loop inside a grounded cylindrical cathode. A permanent magnet is placed so that the cylinder is between its poles and the anode loop is in a plane parallel to the pole faces. Electrons in the chamber are accelerated toward the anode but travel in spiral paths due to the magnetic field. This greatly increases their path length and the probability of ionization and therefore the gauge sensitivity. In this way a current in the milliampere region is produced. This is large enough to be read without amplification. The ionization probability is roughly proportional to the molecular density, so at a fixed temperature the gauge current is an indication of the pressure.

It was found that the discharge gauges are not as accurate as would be desired. Unpredictable jumps of about five per cent occur regularly in the current. This is probably a result of the appearance and disappearance of current leakage paths in the gauge depending on the particular contamination and/or

outgassing properties of the moment. However, it was found that, within these limits, the gauges were reliable over an indefinitely long period of use.

Considering the quality of the results from the discharge gauges, it is pertinent to examine why this type of gauge was chosen. The answer involves the particular pressure range of these measurements. It was necessary to measure pressures as low as 2×10^{-4} mm and as high as 1×10^{-2} mm with roughly the same accuracy. One or the other of these limits falls outside the useable range of all other continuously-reading gauges including: thermocouple, ionization, pirani and alphatron gauges. In addition, the thermal conductivity-type gauges (thermocouple and pirani) have responses which are too slow for the transit time measurements.

The control circuit supplied with the discharge gauge employed a half-wave rectified high voltage of about 5000 volts in series with a resistance of 830 k ohms to the anode. This high voltage would cause the gauge to fire at nitrogen pressures as low as 10^{-6} mm. This series resistance is required not only as a current limiter in case of a short in the discharge tube, but also to drop the potential across the gauge at high pressures. Otherwise the leakage current becomes sizeable. The DC resistance of the gauge itself decreases linearly from about 30 megohms at .01 micron to about 100 k ohms at 1.5 microns. So at pressures below about 0.5 micron the gauge response is

essentially linear, but at higher pressures the response flattens out as the change in gauge resistance becomes small with respect to the series resistance.

Two ways were found in which improvements on the control circuit could be made, at least for the purposes of this experiment. The gauge currents were read as a function of time on a two-channel Sanborn recorder, which picked up the large ripple component of the hali-wave rectified current. This difficulty was removed by simply replacing the gauge power supply by a low ripple, regulated DC supply. Secondly, at a sacrifice of response to pressures below about 10^{-5} mm, the linearity of the gauge in the high pressure region was improved. This was accomplished by lowering the high voltage to 1200 volts which permitted reducing the series resistance to 120 k ohms. This way the gauge response was essentially linear up to about one micron.

The input signal to the Sanborn recorder, Figure 8, was taken from across a ten-turn Helipot potentiometer, which was placed in series in the gauge circuit. The maximum resistance used was 500 ohms, which had negligible effect on the circuit. The linearity of the Helipot over its entire range was verified to be better than the quoted figure of 0.25 per cent. The input impedance of the recorder was 200 k ohms.

The power supply was operated in the floating mode, but

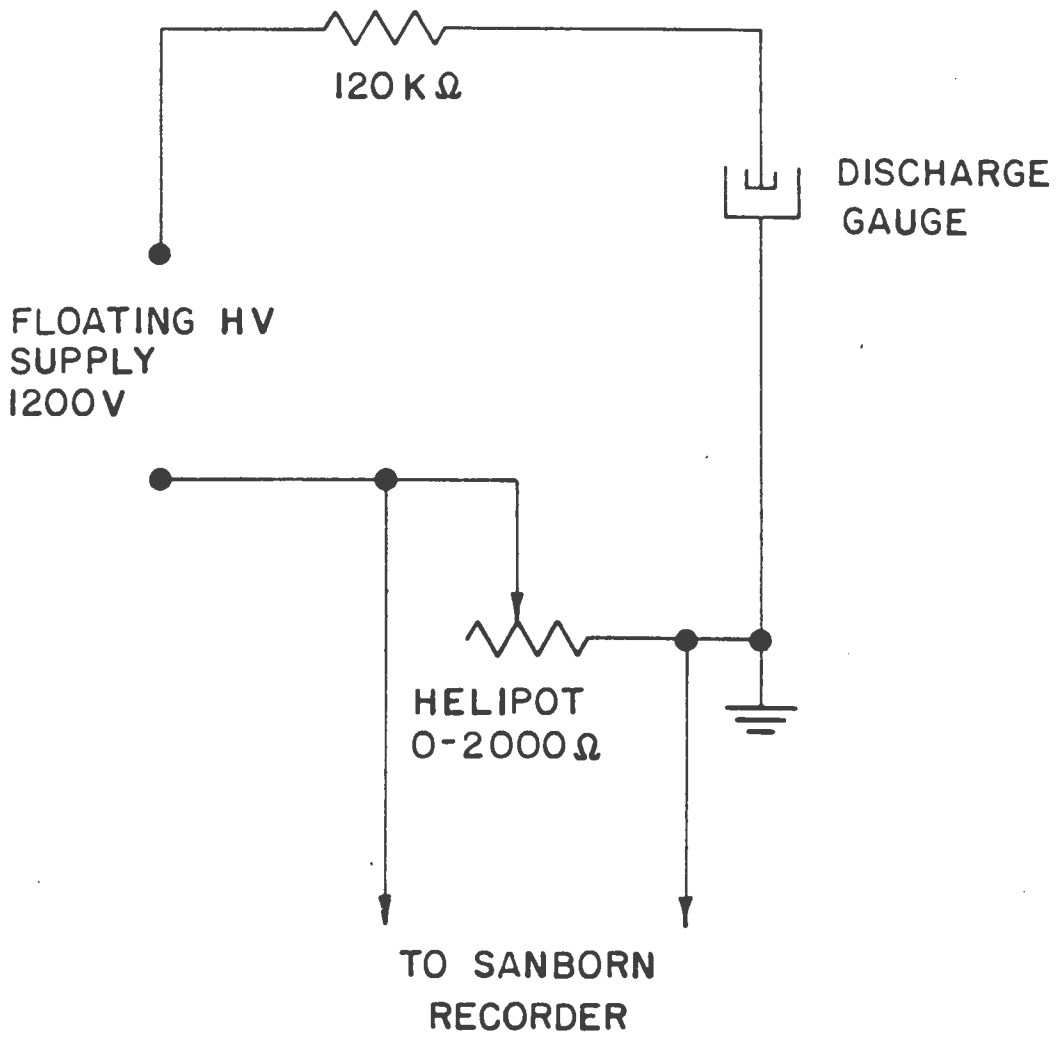

Figure 8. Discharge gauge control circuit

this caused no problem at 1200 volts. The Helipot was then used to keep the recorder reading as near full scale as possible for maximum precision. The gain of the recorder was calibrated before each use, and it was found not to shift over a period of several weeks if the recorder was left on. The precision of the current readings from the recorder was at least one per cent near full scale. The absolute accuracy of the recorder was not important, since the recorder was used for both the calibration and the data runs, but this was nevertheless verified to be within three per cent.

3. General procedure

The calibration curves for the response of the discharge gauges to nitrogen are shown in Figure 9. They have similar shapes, as would be expected for gauges of identical construction, but also significant individuality. The scatter of the points reflects the five per cent limitation already mentioned.

With the gauges at their respective leak-end and pump-end positions the variable leak was adjusted to give sets of readings for P_1 and P_2 over a wide range of pressures under equilibrium flow conditions. This was repeated with nitrogen for each of three different aperture sizes with the results summarized in Table 1 of section I. C.

The calibration curves of the discharge gauges for xenon gas are shown in Figure 10. An anomalous response occurred on

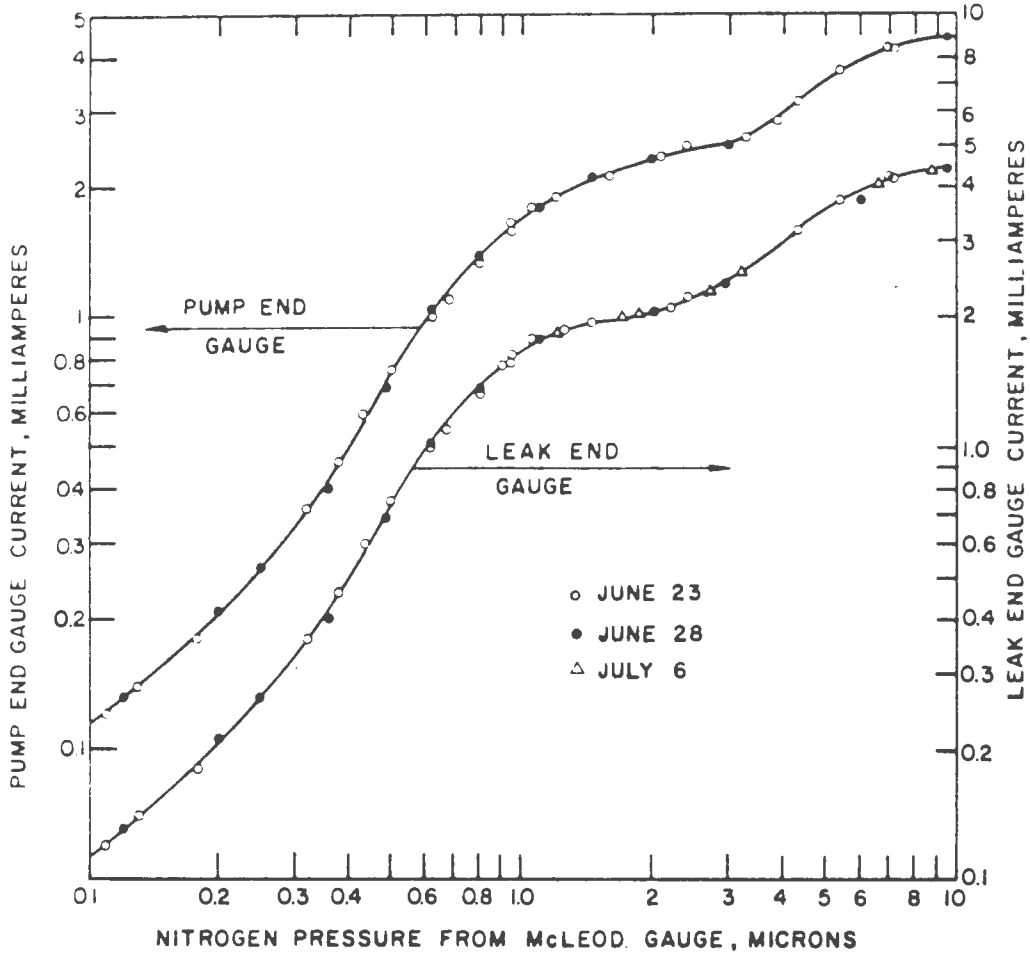

Figure 9. Calibration curves of discharge gauges for nitrogen

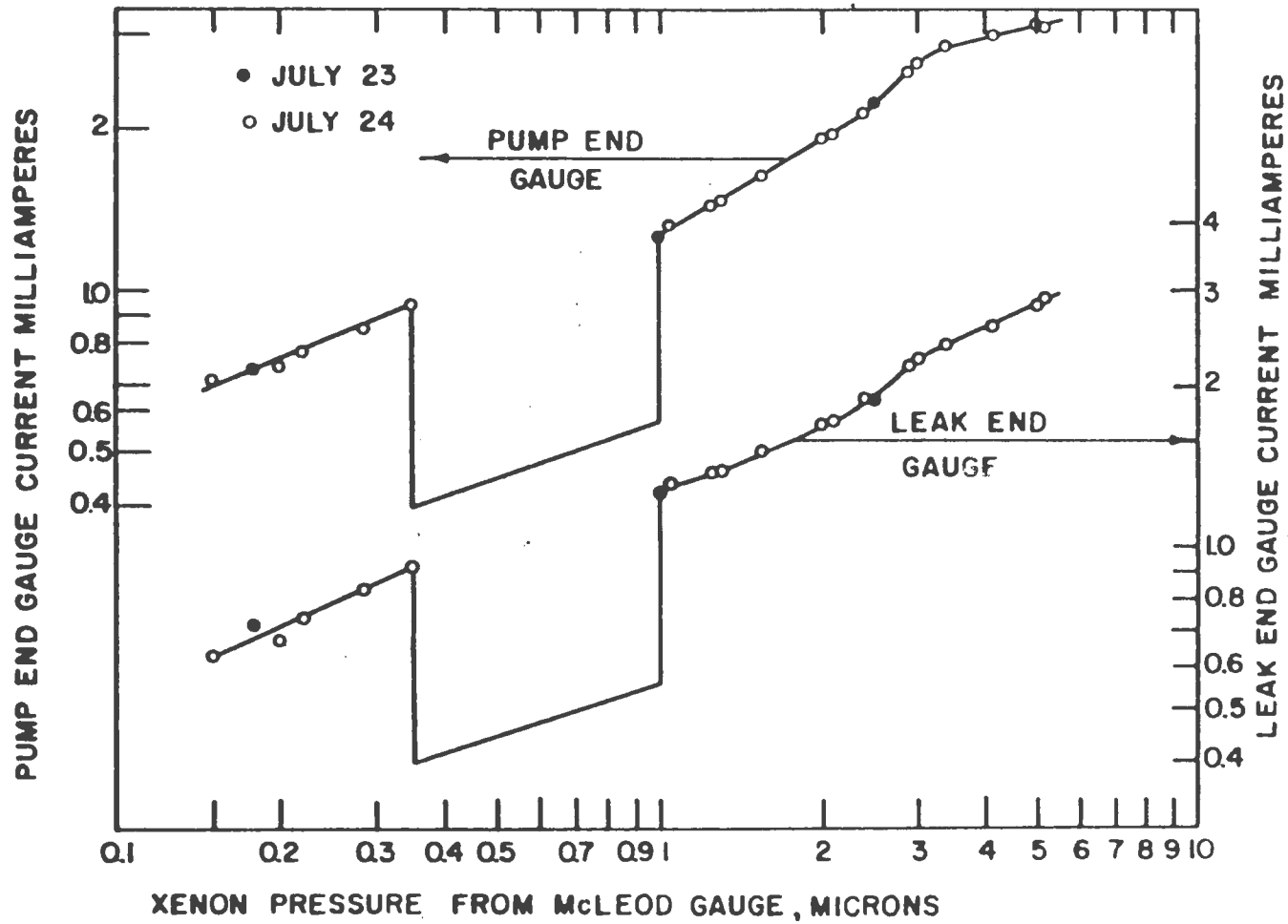

Figure 10. Calibration curves of discharge gauges for xenon

both gauges in the region between about 0.35 and one micron. As seen on the curves this took the form of a sharp discontinuity in current. No explanation can be offered for this anomaly. The gauge current in the lower current state was roughly as shown, but was not reproducible with any degree of precision. These discontinuities prevented obtaining results for the pressure gradient in the low pressure region. However, for higher pressures, where viscous effects are expected to be noticeable, both P_1 and P_2 were measured as for nitrogen.

C. Analysis of Results and Conclusions

The results for the ratio of P_1 to P_2 for nitrogen are presented below.

Table 1. Ratio of P_1 to P_2 for nitrogen

Nominal exit diameter in millimeters	Corrected exit diameter	Number of readings	Measured $\frac{P_1}{P_2}$	Calculated $\frac{P_1}{P_2}$
1.17	1.04	23	2.53 ± .15	2.45 ± .04
1.5	1.35	19	3.54 ± .17	3.46 ± .06
1.8	1.63	17	4.64 ± .26	4.63 ± .07

In calculating this ratio a correction was applied for the thickness of the aperture resulting in the corrected diameter shown in column 2 of Table 1. This is required, because in the derivation of equation 3 molecules coming from all angles are

included. However, in the case of an aperture with finite thickness, those molecules entering the aperture from nearly right angles from its axis will strike the aperture wall. From there they have only a one-half chance of proceeding through the aperture and a one-half chance of returning to the discharge chamber region on their next trajectory. See Figure 11 for this geometry.

The correction factor to express the effective diameter as seen by an approaching molecule depends on Θ and is called $c(\Theta)$. In the figure the entire line-of-sight correction is called $2c(\Theta)$ to account for the remaining one-half chance of still passing through the aperture. The number to be subtracted from the nominal diameter is $\bar{c}$, which is the average of $c(\Theta)$ over all possible angles;

$$\bar{c} = \frac{\int_0^{\frac{\pi}{2}} c(\Theta)\,d\Theta}{\frac{\pi}{2}} = \frac{t\int_0^{\Theta_*} \tan\Theta\,d\Theta + d\int_{\Theta_*}^{\frac{\pi}{2}} d\Theta}{2(\frac{\pi}{2})} \quad . \qquad 24$$

The thickness of the aperature is t and

$$\Theta_* = \tan^{-1}\frac{d}{t} \quad . \qquad 25$$

Performing these integrals gives

$$\bar{c} = \frac{1}{\pi}\left\{ t[-\log\cos\Theta]_0^{\Theta_*} + d[\tfrac{\pi}{2} - \Theta_*] \right\} \quad . \qquad 26$$

Then from equation 17 the ratio of pressures is calculated from

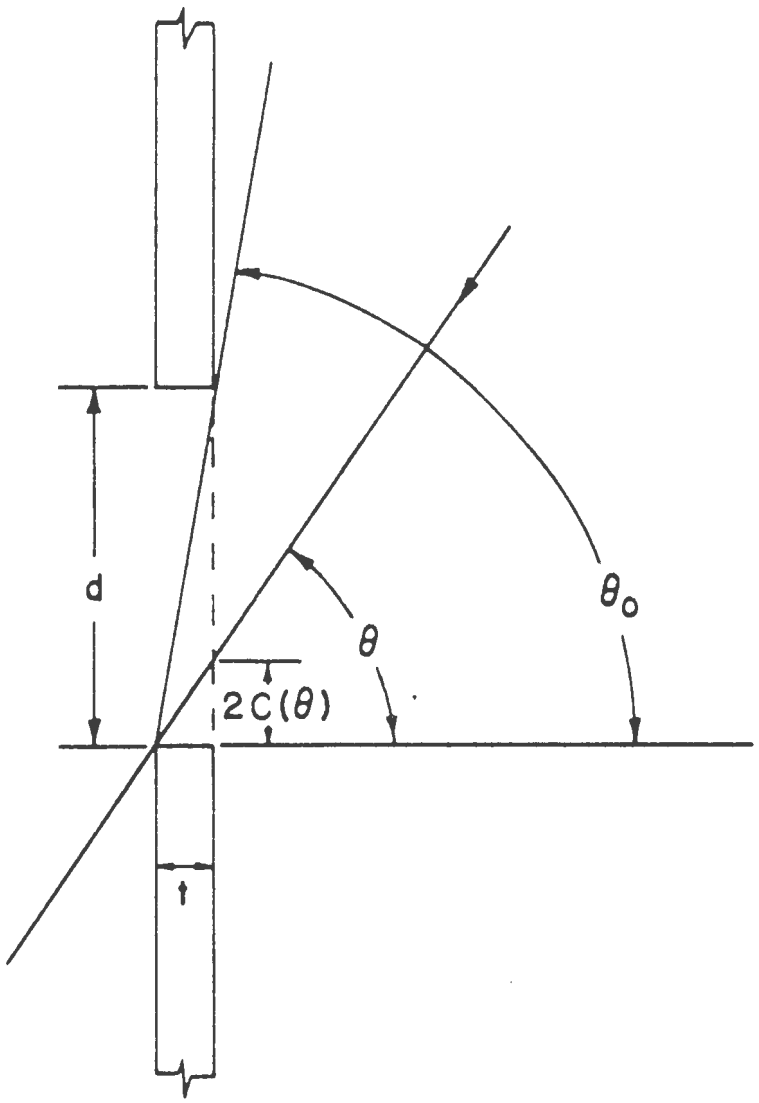

Figure 11. Geometry determining the correction factor for the aperture diameter

$$\frac{P_1}{P_2} = 1 + 1.33\ d_{eff}^2 \qquad 27$$

where

$$d_{eff} = d - \bar{c}\ . \qquad 28$$

The apertures used were made from five mil thick stainless steel. The precision of the hole was about one mil, which determines the error of the calculated ratio. The error quoted for the measured ratio is one standard deviation.

The pressure measurements for nitrogen covered the range from 0.3 to 4.8 microns. The pressure ratio was constant throughout that entire range, showing no deviation, even at the highest pressures, from the ratio calculated on the assumption of pure molecular flow. Some representative points of the ratio for nitrogen are plotted in Figure 12.

The results for the ratio of P_1 to P_2 for xenon with d = 1.17 mm are plotted in figure 12. The solid curve is calculated using $\Delta P = \frac{Q}{C}$ with equation 8, the expression for molecular flow through the small aperture being used for Q, and equation 18 for C. Thus, the viscous effects in the tube are included, but no such correction in the very small aperture is considered necessary. It is unfortunate that points could not be obtained over a greater pressure range, but those which were obtained agree with the calculated curve to well within the five per cent error, and they show a small, but definite, viscous effect.

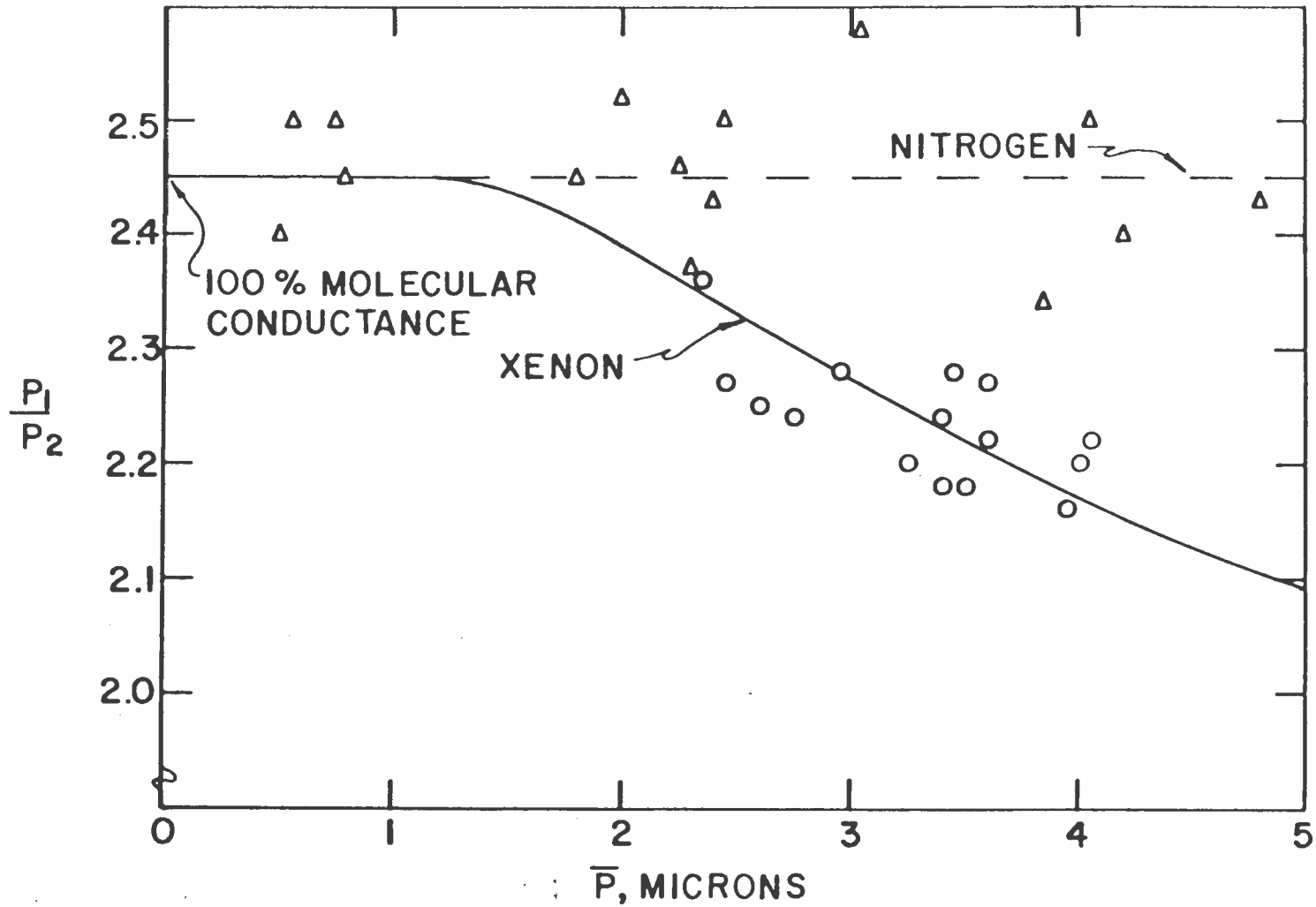

Figure 12. Ratio of P_1 to P_2 for d=1.17 mm for nitrogen and xenon; the lines are calculated.

These results show that the pressure ratio in the transport line may be calculated from simple molecular flow theory even though λ is of the order of, rather than much greater than, D. Under these conditions the ratio depends only on the geometry of the line and the exit aperture. It is particularly useful that the ratio does not depend on the pressure and the temperature, because these parameters, especially the exact pressure of a hot, radioactive gas, would be difficult to supply to the computer controlling the steady-state activation system. The results for xenon show that even a heavy gas at the highest ion source pressures may be treated as essentially obeying molecular flow with a small viscous correction.

III. TRANSIT TIME

A. Theoretical Study

In attempting to calculate the transit time of molecules down the transport tube the molecular flow approach used in section II will be continued.

The general three-dimensional form of equation 10 is

$$\frac{\vec{Q}}{A} = -\mathcal{D}\vec{\nabla} n \quad .$$

Taking the gradient of both sides gives

$$\vec{\nabla} \cdot \frac{\vec{Q}}{A} = -\mathcal{D}\nabla^2 n$$

if $\mathcal{D} \neq \mathcal{D}(x,y,z)$. This is justified under molecular flow conditions, because in that case from equation 11

$$\mathcal{D} = \frac{1}{3} \bar{v} D \quad .$$

From the equipartition theorem $\bar{v}$ is a function only of temperature and not of any linear dimension. The equation of continuity, with $\frac{\vec{Q}}{A}$ representing the particle current density, is

$$\vec{\nabla} \cdot \frac{\vec{Q}}{A} + \frac{\partial n}{\partial t} = 0$$

from any text on theoretical physics (e.g., 9, p. 187). Combining equations 25 and 27 gives the diffusion equation

$$\frac{\partial n(x,t)}{\partial t} = \mathcal{D} \frac{\partial^2 n(x,t)}{\partial x^2}$$

in the case of the transport line where the only particle

gradient is in the x direction. A solution of this equation is (10, p. 156)

$$n(x,t) = \frac{\text{constant}}{[4\pi\mathcal{D}t]^{\frac{1}{2}}} e^{\frac{-x^2}{4\mathcal{D}t}} . \qquad 29$$

It is desired to have the distribution function f(x,t) which, by definition, is normalized to unity over the range of x = 0 to ∞. It is related to n(x,t) by a normalizing constant. For the present purposes x = 0 is chosen at the port shown in Figure 6 for the calibration of discharge gauge number 2. It will be assumed that, due to the experimental arrangement, all negative x coordinates are forbidden to the molecules. In fact, there is a small volume available to the diffusing molecules on the negative side of x = 0. However, this is unimportant with respect to the volume from x = 0 to ∞, and only serves to raise the tail of the diffusion curve very slightly. Then requiring that

$$\int_0^\infty f(x,t)dx = 1 \qquad 30$$

gives for the distribution function of the molecules

$$f(x,t) = \frac{2}{[4\pi\mathcal{D}t]^{\frac{1}{2}}} e^{\frac{-x^2}{4\mathcal{D}t}} . \qquad 31$$

This is the well-known Gaussian distribution function. At t = 0 it has the behavior of the Dirac delta function, which is zero everywhere except at x = 0 where it is infinite, and its integral over all x is unity (7, p. 65).

The mean squared displacement of a molecule in the x

direction is

$$\overline{x^2}(t) \equiv \int_0^\infty x^2 f(x,t)dx = 2\mathcal{D}t \ . \qquad 32$$

Substituting equations 26 and 5 and solving for t gives

$$t_{peak} = \frac{3x^2}{2D}\left[\frac{\pi m}{8kT}\right]^{\frac{1}{2}} \qquad 33$$

where t_{peak} is the time at which the distribution function at x reaches its peak value. In the following "transit time" will be synonymous with t_{peak}. This result is also obtained by simply maximizing equation 31 with respect to time at constant x. The distance x for these measurements was 355 cm. The distribution of molecules as a function of time at this coordinate following a delta function of nitrogen molecules applied at x = 0, t = 0 is

$$f(355,t) = \frac{e^{\frac{-1.55}{t}}}{252[t]^{\frac{1}{2}}} \ . \qquad 34$$

This function is plotted in Figure 13.

The transit time as calculated from equation 33 is 3.1 seconds for nitrogen and 6.73 seconds for xenon. These results are again based on molecular flow conditions. There is no question about the validity for pressures low enough that the strict molecular flow criterion is fulfilled. However, as seen in Section II, the transport line operates at pressures such that λ is of the order of D. This means that a significant

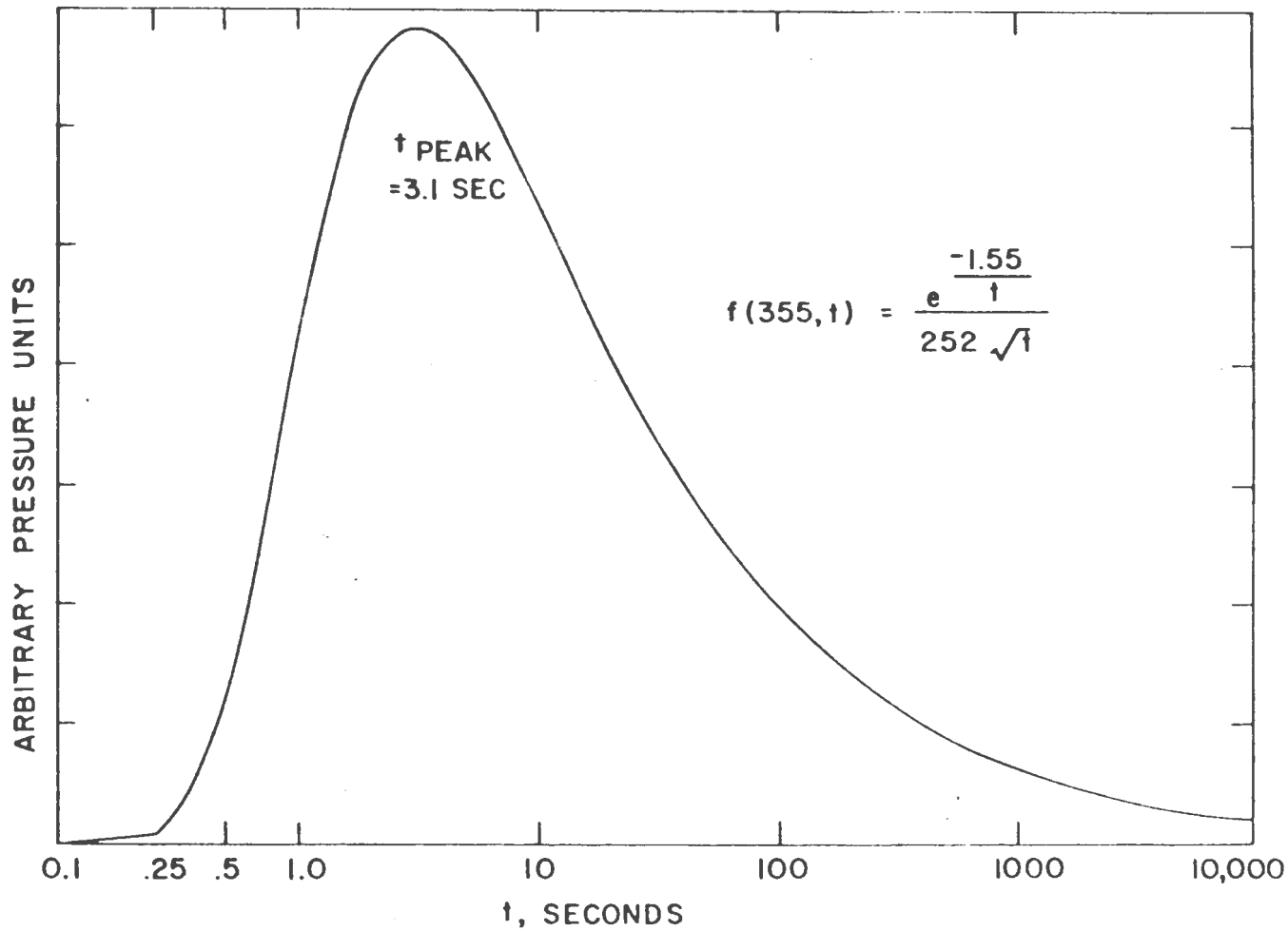

Figure 13. Calculated pressure as a function of time at x=355 cm after a delta function of nitrogen at x =0, t=0.

number of collisions will not be diffuse reflections from the tube wall, but will be collisions of two molecules in which, of course, their total momentum is conserved. Since the net flow of molecules is down the tube in the direction opposite the particle density gradient, there is a net momentum in this direction. So if, on the whole, there occurs some momentum conservation for the molecules, it is predominately in this direction. Then it follows that, if in a molecule's journey down the tube a significant portion of the collisions it suffers are with other molecules rather than with the walls, the transit time will be somewhat decreased.

This argument is limited to pressures well below those for which the flow is purely viscous. The molecules, although occasionally colliding with each other, must still move essentially independently. For an example of this limit, at $\bar{P}$ = 500 microns nitrogen flow is ninety per cent viscous from equation 18. The argument would probably not apply in this region. For viscous, or mass, flow the fluid moves at equilibrium essentially as a plug, and for a given molecule to pass through the aperture all the molecules in front of it must precede it through. In this case the average transit time of a molecule is just the volume of the system divided by the pumping rate of the aperture. For nitrogen this is about nine seconds when d = 1.5 mm. This clearly shows that the argument of molecular collisions speeding the transit cannot apply for

pressures much above those for which λ is of the order of D.

Measurements of the transit time for nitrogen and xenon were conducted to check the molecular flow transit time and to determine the effect which results from pressures in the transport line exceeding the molecular flow criterion.

B. Experimental Investigation

For the measurement of transit time the gas flow through the transport line was adjusted to the desired value with the variable leak. Then what was essentially a delta function of molecules of the same gas was superimposed on this equilibrium flow. The arrival of this pressure pulse at the ion source end of the line was noted with the discharge gauge.

The delta function of molecules was created by a fast-acting toggle valve joined directly to the transport line at the third port on the leak end of the system. On the other side of this valve was tubing to the gas bottle. A provision was included to pump out part of the gas in this tubing so the magnitude of the pulse could be controlled.

The mark for t = 0, the moment of flipping the toggle switch, was provided by the leak-end discharge gauge. This gauge was located about 18 cm from the valve opening. The distribution function of molecules diffusing to this gauge is f(18,t) from equation 31. This function has the same shape as the one plotted in Figure 13, but has a peak at t = 0.008 seconds. Due to the increased pressure in the area at the time

of a pulse, intermolecular collisions probably make t_{peak} somewhat less than this. The time at which f(18,t) begins to increase rapidly, corresponding to t = 0.25 second for f(355,t) in Figure 13, is about t = 0.0007 second. For the purposes of this experiment, this time which was very definite on the recorder output, served nicely as a mark of t = 0. The rise time of the current as read by the recorder to one-half maximum was about 0.02 second. This was not fast enough to record the peak at the leak-end discharge gauge, but is certainly sufficient for the measurements of diffusion to the ion source end of the transport line.

The fast-acting valve shut off the supply of molecules at least as fast as it was turned on. This created a delta function, at least on the time scale of these measurements, of molecules at x = 0, t = 0 as desired. This does not mean, however, that the pressure dropped back to its original value immediately after the delta function was applied. Due to the diffusion properties of the molecules, the pressure at x = 0 remained higher than at t = 0 for many seconds. Indeed, it was this characteristic of the molecular motion that was of interest.

Delta functions of various magnitudes for xenon and nitrogen were superimposed on the equilibrium flow at various values of $\bar{P}$. By plotting the transit time to the pump-end discharge gauge as a function of the magnitude of the pulse

and extrapolating to a pulse of zero magnitude, the transit time of molecules in equilibrium flow was obtained.

C. Analysis of Results and Conclusions

The typical response of the pump-end discharge gauge to nitrogen delta functions at $x = 0$, $t = 0$ is shown in Figure 14 compared to $f(355,t)$. In the graph all curves have been normalized to the same peak pressure for the purpose of comparison.

Curves number one and two are the result of delta functions superimposed on an equilibrium flow with $\bar{P} = 0.23$ micron. The peak pressure P_1 was 0.8 micron for curve number one and 2.7 microns for curve number two. It will be noticed that no discernible deviation of t_{peak} from that for $f(355,t)$ occurred in either of these cases, yet some differences in the response were noticeable for t greater than about five seconds.

The difference at large times of curves one and two from each other and from the calculated $f(355,t)$ is attributed to intermolecular collisions occurring along the transport distance. The peak pressures in both cases were high enough to expect some effect due to this occurrence. That t_{peak} is not altered is explained by the fact that those molecules which are among the first to arrive at the other end have traveled the most direct route with relatively few collisions with either the tube wall or other molecules and are therefore relatively

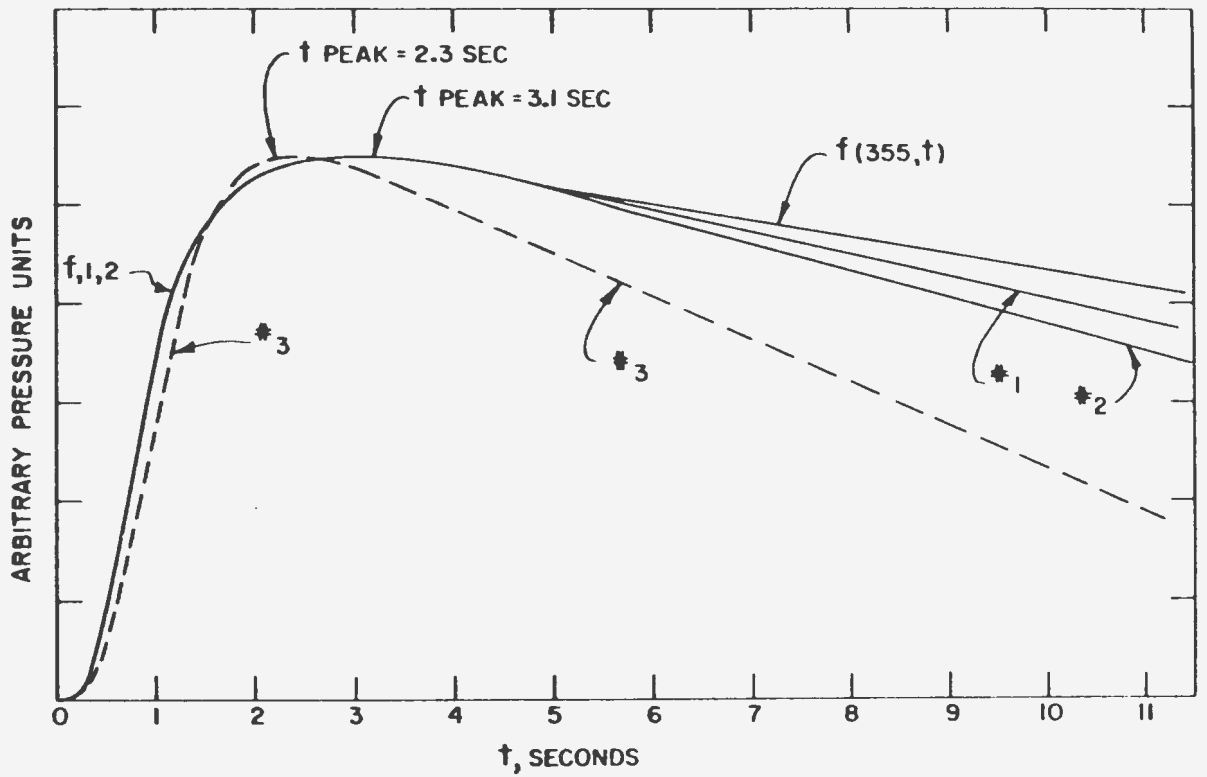

Figure 14. Calculated and measured pressures at x=355 cm following a nitrogen delta function at x=0, t=0.

immune to the small viscous effect.

Curve number three was obtained with $\overline{P}$ = 4.8 microns. The peak pressure P_1 was off scale, whereas that for P_2 was 5.8 microns. In this case the pressures were great enough to significantly affect t_{peak} as well as the total flow. This pattern of effects was consistent throughout the measurements.

Figure 15 shows the results for the peak transit time of nitrogen as a function of the peak pressure P_2 resulting from a delta function pulse. Only for the broken curve, with $\overline{P}$ = 4.8 microns, was the equilibrium pressure high enough to be able to observe an effect in the transit time due to $\overline{P}$ alone. The "x" at the extrapolated end of the curve denotes P_2 and t_{peak} at equilibrium flow conditions. In this case the transit time was 2.95 seconds. In all other cases, regardless of $\overline{P}$ at equilibrium, extrapolation to zero delta function gave a transit time of 3.1 seconds. Consequently, no distinction was made in the figure as to the various equilibrium pressures, and all points are given alike as dots. It was the magnitude of the delta function in these cases which determined t_{peak}.

No difference in the transit time is seen in the molecular flow region when the exit aperture diameter is changed. This is expected because equation 33 does not depend on d. For large P_2 where viscous effects are noticeable the exit diameter does affect the transit time, simply because, from equation 17, a larger d means larger P_1 for a given P_2 and therefore a

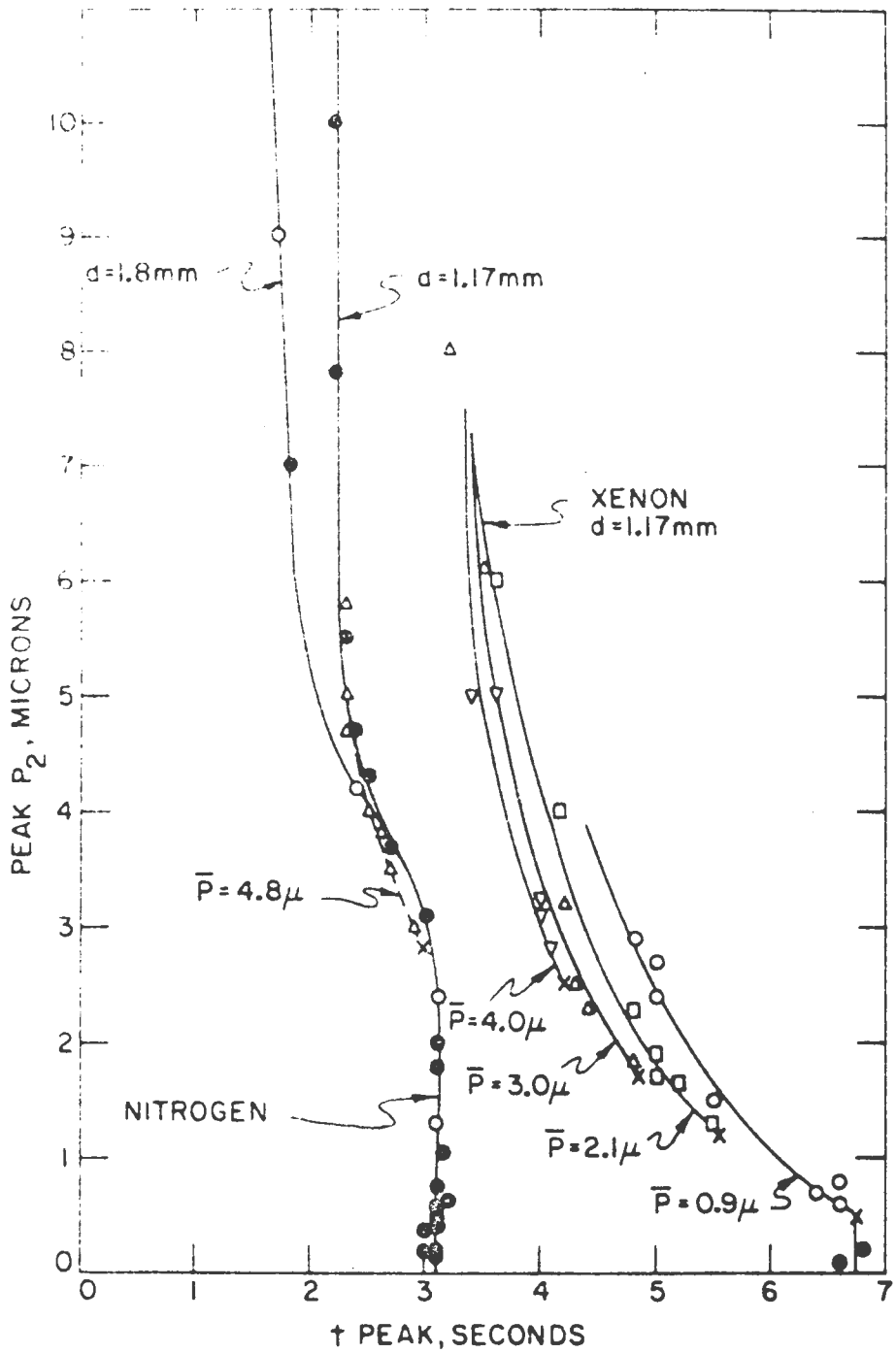

Figure 15. Transit time as a function of $\bar{P}$ and the peak P_2 pressure.

larger viscous effect.

Figure 15 also shows the peak transit time for xenon as a function of the peak P_2 and $\overline{P}$. Again the "x" at the end of each extrapolated curve denotes the transit time and P_2 at equilibrium flow for that particular $\overline{P}$. The lowest three points on the $\overline{P}$ = 0.9 micron curve were obtained with the pump-end discharge gauge in the lower current state, as mentioned in Section I.B.3. Consequently, the pressure indicated is only approximate. The two lowest points were obtained at very low pressures where molecular flow was assured. They confirm that the locus of transit time points as $\overline{P}$ is decreased does not continue to increase but remains constant at 6.7 seconds. This and the transit time for nitrogen agree with the calculations from equation 33.

Figures 14 and 15 show that the transit time of a molecule through the transport line can be calculated on the assumption of molecular flow even though the pressures involved are such that the strict criterion for molecular flow is not satisfied. At a $\overline{P}$ of about 4.8 microns for nitrogen and about 1.5 microns for xenon the equilibrium flow transit time begins to show the effect of intermolecular collisions, causing the transit time to be slightly decreased.

IV. ELECTRICAL DISCHARGE

A. Background

In this section the problem is to study the dependence of the onset of electrical discharge in a gas on mean free path (or pressure), voltage and gap length for the particular configuration presented by the transport line with a short insulating section of tubing in the line. The idea here, as pointed out in the introduction, is to be able to have the reactor end of the transport line at ground potential while the ion source end is at the accelerating potential of about 60 kV.

A vast body of literature on gas discharge exists, but nothing could be found dealing with the low pressures, high potentials and particular geometry dictated by the transport line. For example, Paschen's Law, which has been the guidepost of most gas discharge work since 1889, does not hold in this region. This law states that in a uniform electric field the sparking potential is a function of the product $P_G L_G$ and not of P_G and L_G separately (4, p. 293; 5, p. 32). The sparking potential V_S is defined as that potential at which a non-self-sustaining (Townsend) discharge becomes self-sustaining. P_G is the gas pressure (at constant temperature) and L_G is the gap length.

This product is, of course, just proportional to the number of molecules available in the gap to conduct charge during a

discharge. The law does not hold for P_G less than about 0.5 mm Hg or L_G less than 1 mm. It cannot hold for vanishingly small P_GL_G, because this would imply that V_s goes to infinity, but breakdown is known to be possible even at ultra-high vacuum and certainly for vanishingly small gaps. The pressure in the gap in the transport line will be on the order of one micron (10^{-3} mm), so Paschen's Law cannot be used to determine V_s.

A study has been conducted recently by Maitland (11) on the effect of pressures on breakdown in the so-called vacuum insulation region. This is the pressure region below one micron where breakdown is supposedly entirely independent of the gas pressure and depends only on the potential and the nature of the electrodes. He has found some small pressure dependence, due mostly to the effect of the gas on the surface of the electrodes. Again these results are not applicable to the transport line, because this study revealed that the gap pressure was still high enough to be very important in determining V_s.

In addition the electric field in the gap resulting from end-to-end cylinders is non-uniform, making it even more unlikely that any previous study would have encompassed all the necessary conditions of this problem.

The mechanism of the Townsend discharge will prove helpful in understanding some of the results of this study, although the name "Townsend discharge" accurately applies to a low voltage discharge in a gas of pressure of a few millimeters.

It can be described qualitatively in the following way (4, pp. 270-279; 5, pp. 26-31): A small, but ever-present number of free electrons are created in the gas by background radiation. If a potential greater than the first ionization potential of the gas is applied to the gap, the electrons are accelerated and, being efficient ionizers, they create more electrons on their way to the anode. These electrons do the same leading to an avalanche of electrons to the anode. However, this process is not sufficient to explain the currents of perhaps a microampere which are observed in such a discharge (5, p. 28). Positive ions created in addition to the initial electrons are accelerated by the field to the cathode. They cause very little ionization by collision on the way to the cathode because of their relatively large mass, but upon striking it they may liberate electrons. Each of these electrons may initiate another avalanche, and so on. This process leads to the Townsend discharge current of a few microamperes for an applied potential of 50 to 100 volts. The current increases with increasing voltage until the sparking voltage is attained. At this voltage, by definition, the discharge becomes self-maintaining; meaning the original source of electrons and ions could be removed and the discharge would continue. Thus, at this voltage each secondary electron leaving the cathode is able to produce enough ionization that the resulting positive ions in returning to the cathode will produce one electron. At voltages

above V_S breakdown occurs leading to a drop in voltage across the gap and currents in the milliampere region.

A similar process occurs in the transport line gap, even though the pressures are much lower and the voltages much higher. To some degree the results may be understood with this picture.

B. Experimental Investigation

The transport line used for sections II and III was also employed for these measurements. A three foot long section was removed from the copper tube and vacuum flanges soldered on the two open ends of the line. Three gap assemblies, as illustrated in Figure 16, were constructed, one each of gap length L_G of two, four and seven inches. The insulating gaps were pyrex glass tubing 16 mm O.D. and 11 mm I.D. An inside diameter slightly less than that of the copper tubing was chosen, so line-of-sight arcing between the copper sections was eliminated. Glass gaps were used to permit visual observation of the discharge. Both the mechanical and vacuum connections of the end-to-end sections of copper and glass were made with epoxy resin as shown in the figure. In the final transport line to the separator ion source there will be only one such gap, since the ion source end of the line will be at 60 kV. However, for this study in order to keep both ends of the transport line and all associated equipment at ground potential, two identical gaps were used with the positive potential being

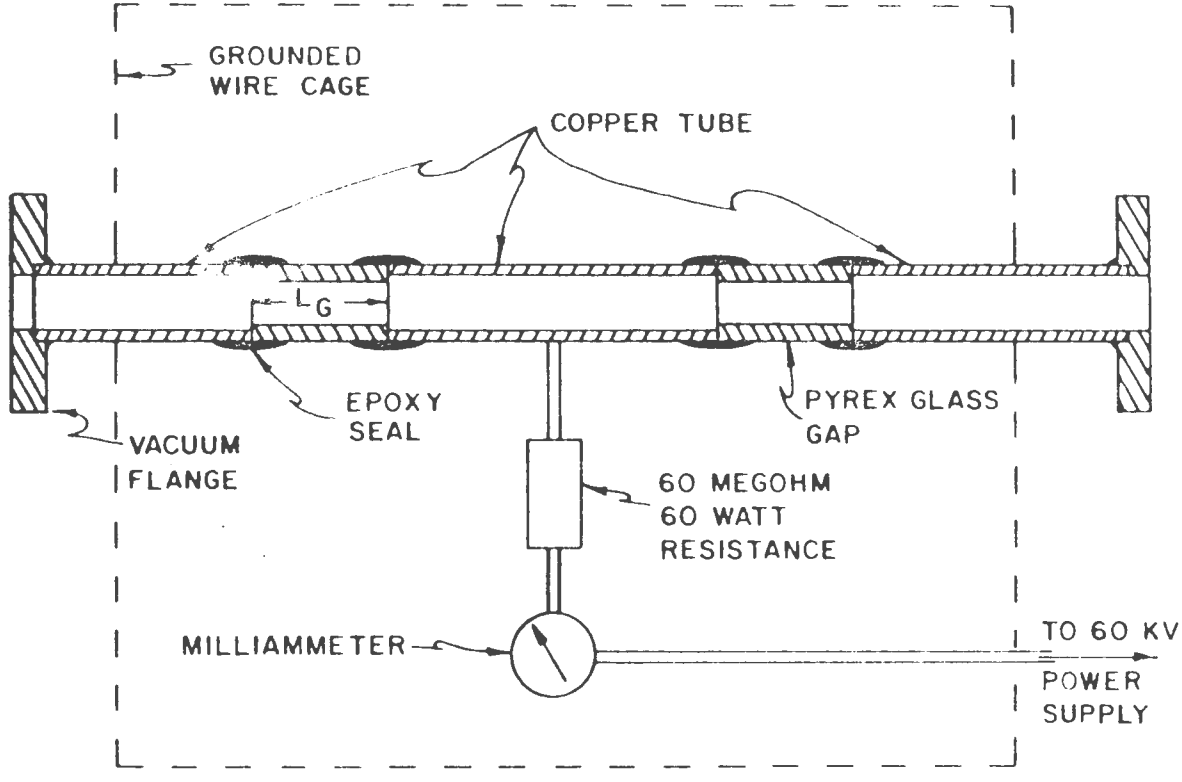

Figure 16. Schematic of discharge gap assembly.

applied to the copper section between these gaps. During the measurements all discharges were seen to be initiated first in the higher pressure gap as expected, so all results will be discussed in terms of it.

A sixty kilovolt, one milliampere DC power supply provided the high positive potential to the center copper section through a current meter and a sixty megohm, sixty watt resistance whose purpose was to limit the current at breakdown to one milliampere. Both ends of the transport line were grounded, and for safety the entire apparatus was surrounded by a grounded wire cage.

As in the previous measurements, the equilibrium gas flow in the transport line was established at the desired value with the variable leak. The pressures encountered at gas discharge were too high to measure accurately with the discharge gauges, so the McLeod gauge located at its port as shown in Figure 6 was used. With equilibrium flow in the line, pressure P_1 was measured with the McLeod gauge. Then the voltage across the discharge gaps was slowly increased until the sparking voltage V_s was reached. This was repeated several times to insure a correct reading for V_s, then P_1 was rechecked to insure it had not changed.

It was seen in Section II that at high pressures the conductance C of the transport line shows some effects due to viscosity. This must be considered in the calculation of P_G from

P_1. For an exit aperture effective diameter of 1.04 mm, which was used for most of the gas discharge work, from $\Delta P = \frac{Q}{C}$ and equation 8 the result for nitrogen is

$$\Delta P = \frac{101\ P_2}{C} \qquad 35$$

if C is in cc per second. Equation 18 which includes viscous effects in the tube is now to be used for C. This equation is still linear in the length of the tube L, so

$$P_G = P_1 - \frac{231}{363}\ \Delta P \qquad 36$$

where 231 cm is the distance between P_1 and P_G, and 363 cm is the distance between P_1 and P_2. Using equation 35 and

$$P_2 = \frac{P_1}{1 + \frac{101}{C}} \qquad 37$$

gives from equation 36

$$P_G = P_1 - \frac{63.7\ P_1}{C + 101}\ . \qquad 38$$

To find C which is expressed as a function of $\overline{P}$ in equation 18 and Figure 5 it was necessary to find $\overline{P}(P_1)$. For pure molecular flow this is simply $\overline{P} = 0.70\ P_1$, but when viscous effects are included it is a function of C also, so a graphical solution was required. From the definition of $\overline{P}$ upon substituting equation 37 and solving for P_1 one obtains

$$P_1 = 2\overline{P}\ [\frac{C + 101}{2C + 101}]\ . \qquad 39$$

Plotting this as a function of $\overline{P}$ gives the required $\overline{P}(P_1)$ to obtain C for use in equation 38.

Similarly for xenon with d_{eff} = 1.04 mm the results are

$$P_G = P_1 - \frac{29.8\ P_1}{C + 46.9} \qquad 40$$

and

$$P_1 = 2\overline{P}\ \left[\frac{C + 46.9}{2C + 46.9}\right] . \qquad 41$$

These relations for P_G give a significantly larger value of P_G (up to thirty per cent for xenon at the highest pressures) for a given P_1 than that calculated from simple molecular flow.

C. Analysis of Results and Conclusions

The voltages and pressures at which self-sustaining gas discharge was observed in nitrogen and xenon are shown in Figure 17. Above and to the right of each curve is the region of continuous discharge; below and to the left is the region of no self-sustaining discharge. The up and down triangles for the four inch nitrogen curve were obtained on different days using different-sized exit apertures. The agreement of the points attests to their reliability. The results for the two inch gaps with nitrogen were not reproducible above about 20 kv. This seems to have been due to increased sparking which could have increased the pressure locally to an extent depending on the outgassing condition of the tube.

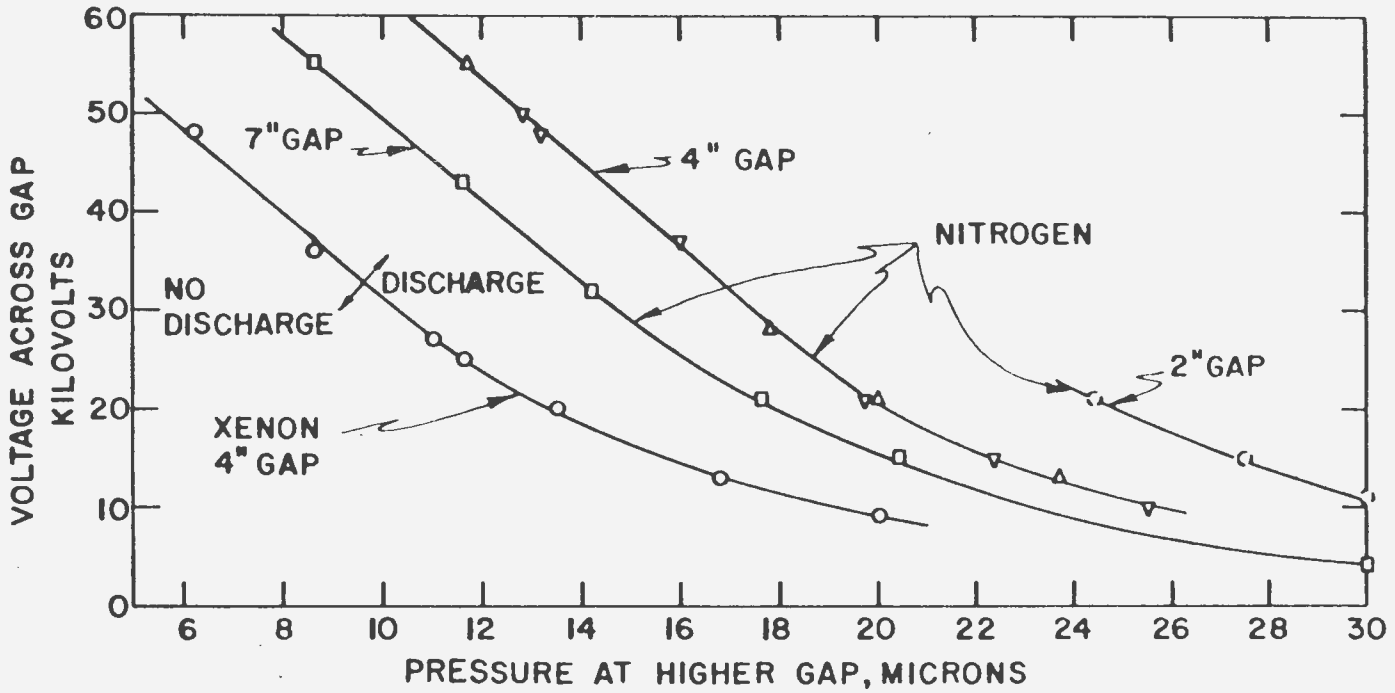

Figure 17. Gap voltage and pressure at discharge.

At voltages less than V_s the meter registered small currents of perhaps 0.05 ma at 30 kV and 0.1 ma at 60 kV for the four inch gaps. These currents were attributed to leakage across the outside of the glass as opposed to charge motion within the gas, because such a leakage current could actually be seen with the eye. Also when the gas inside was at about 10^{-5} mm pressure, the so-called vacuum insulation region, the current persisted. In the final transport line the gaps would not need to be transparent, and could be constructed of a thick dielectric which would eliminate this leakage current. Undoubtedly some Townsend-type discharge would remain causing a very small and unimportant load on the acceleration power supply.

At voltages less than V_s pulses of gas were transported down the tube and through the electric field at the gaps. There was no noticeable effect on the transit time nor any disturbance of the gas flow by the field.

At high pressures such that V_s was less than 30 kV the onset of self-sustaining gas discharge occurred at a very well-defined voltage. Below V_s there was no visible activity at all in the gap and at exactly V_s the discharge began. At high pressures the glow is a deep red color for both nitrogen and xenon and it fills the entire volume of the gap uniformly.

Within a few volts of V_s when V_s was above about 30 kV some spontaneous sparking occurred in the gaps. The magnitude of

the current in these sparks is not known, but they are of such short duration and infrequent enough that they should not be disruptive to the production and deposition of a steady ion current by the isotope separator. This sparking increased until V_s was reached. This was marked by the appearance of the glow and the current increasing so that it was limited only by the external resistance. In this range the nitrogen glow was bluish in color and the xenon glow was gray. They were to some degree focused in the center of the gap. This was apparently due to the non-uniformity of the electric field. At no time was any structure of the glow observable as in the case of the high pressure glow discharge between parallel plate electrodes, which exhibits the Crookes and Faraday dark spaces, negative glow and positive column (5, p. 42).

This self-sustaining gas discharge cannot be allowed to occur in the transport line during steady-state isotope separation and analysis runs for two reasons: First, the voltage across the gap falls to almost zero during discharge. This would ground the accelerating voltage causing loss of the ion beam. Secondly, the gas discharge operates as an ion pump imbedding the ions in the walls of the tube and causing a drop in pressure at the ion source end of the transport line.

An attempt will be made to explain the shape of the curves of Figure 17 in terms of the Townsend discharge culminating in complete electrical breakdown at V_s as outlined in Section IV. A. It is known that electrons and positive ions are always

present in the gap due to the background radiation. At P_G of about 30 microns enough molecules are present in the gap to support easily a discharge, so V_s does not change much with a change in P_G. However, as P_G is decreased, causing λ to increase, ionizing collisions by the electrons become more infrequent. Then for a discharge to be initiated it is up to the positive ions to create more secondary electrons at the cathode. This they do increasingly well as their energy is increased, so at lower pressures V_s changes more rapidly with P_G. So in this region, and especially at even lower pressures than encountered here, the number of primary ion pairs is not as important as the effectiveness of secondary electron production.

The relation of the curves to each other cannot be explained quantitatively. This is not unusual in gas discharge work. The best that can be done is to suggest that the four inch xenon curve occurs at lower pressures than the corresponding nitrogen curve because the ionization probability for xenon at a given pressure is greater than for nitrogen. This is due to the larger molecular diameter giving a smaller mean free path from equation 6 and a smaller first ionization potential. The molecular diameters are 3.75×10^{-8} and 4.91×10^{-8} cm for nitrogen and xenon respectively (12, p. 36), and their ionization potentials are 16.7 and 12.1 volts. The seven inch nitrogen gap discharges at lower V_s than the four inch gap at a given P_G, because more ionizing collisions occur within the influence of

the electric field. Note, however, that Paschen's Law does not hold in this range, so there must be more to the explanation than just this.

Since the ion source of the isotope separator at the end of the transport line has a maximum operating pressure of 1.5 microns, the maximum P_G will be 2 to 2.5 microns. From the above data the conclusion can be drawn that there is a good chance of being able to apply the 60 kV gradient to a four inch gap in the line and avoid a gas discharge.

V. APPLICATIONS OF RESULTS

The final objective toward which the results of this study will be directed is the design and construction of the most effective possible transport line to deliver molecules from the reactor core to the ion source of the electromagnetic isotope separator. Some of the criteria of this line can be specified from the results of this study.

From the results of Section II it can be calculated that with an effective exit aperture diameter of 1.35 mm, which is about the case for the ion source supplied with the separator, and a tube diameter D of one-half inch, P_1 must be kept at 5.0 microns to maintain the ion source pressure at its maximum of 1.5 microns. The rare-earth elements are of particular interest for analysis by the described system. They are quite non-volatile, so it becomes of interest to determine the temperature required at the reactor end of the transport line to maintain the required pressure of five microns. Nielsen (1) gives the approximate temperatures of the rare-earth metals and their chlorides corresponding to this pressure. This data is presented in Table 2. This shows that for all elements except four a significantly lower temperature will suffice if the chloride form is employed.

The required P_1, and therefore the temperature of the transport line, may be substantially reduced according to

Table 2. Temperatures required for a vapor pressure of five microns for the rare-earth metals and their chlorides

Rare-earth element	Metallic form (°C)	Chloride form (°C)
La	1580	690
Ce	1480	710
Pr	1300	700
Nd	1230	700
Pm	770	770
Sm	320	850
Eu	230	850
Gd	1210	690
Tb	1200	650
Dy	920	650
Ho	1200	620
Er	1120	620
Tm	720	620
Yb	370	790
Lu	1470	620

equation 15 if a tube with a larger diameter D is used. The diameter cannot be increased without limit, however, because of the required radiation shielding in the reactor beam tube. This sets a practical upper limit on D of perhaps one inch. The maximum P_1 would then be about two microns allowing a decrease in temperature.

Doubling the diameter of the tube also shortens the transit time, which is a desired feature. An average rare-earth chloride (all but samarium are trichlorides) has a molecular mass m of about 265. Assuming the required temperature is about 600°C leads to a transit time from equation 33 of 2.75 seconds in a one inch diameter tube.

The transport line will have to come through the beam tube in the form of a slow spiral or helix, so that no direct path will exist for neutrons to escape from the reactor core. This shape will not affect the calculated transit times (as long as the increased path length is considered) because in the molecular flow region, which has been shown to be the case in the transport line, corners or bends do not affect the flow.

In regard to the gas discharge problem, the decrease in P_G, for a given ion source pressure, due to a larger tube diameter would lessen the chance of discharge. The higher temperature required for the rare-earth chlorides will roughly compensate for their larger molecular diameters in equation 6 for the mean free path λ. A problem that has not been considered so far is that the gas passing through the gap in the operational transport line will be radioactive. Assuming that P_G is about two microns the number of molecules per cc at that point will be 2×10^{13} from equation 7. A typical value for the ratio of activated to unactivated atoms is 10^{-7}. If a one inch diameter four inch long gap is used, there will be

about 10^8 radioactive atoms in the gap at every instant. For a half-life of ten seconds the activity in the gap will be 7×10^6 disintegrations per second. These will be beta decays, each creating a high energy electron and a recoil ion within the influence of the electric field. Due to the low pressure the electrons will be relatively ineffective in producing further ionization, and as seen in Section IV the initiation of a gas discharge will be largely dependent upon the ability of the positive ions to produce large numbers of secondary electrons, which depends on the applied voltage. So it can be argued that the increase in the number of primary ion pairs in the gap due to radioactive decay may not be sufficient to lead to a discharge, and that the initiation of such in low pressures still would require the application of a voltage greater than 60 kV as in Figure 17.

This viewpoint is best considered as an argument for conducting further investigations on the electrical discharge properties of the gap in the transport line when the gas used is radioactive. The present study holds out hope for being able to handle the voltage gradient problem with a short insulating section in the transport line, but it seems improbable that the problem can be completely solved without trying it under the true experimental conditions.

VI. LITERATURE CITED

1. Nielsen, K. O. The development of magnetic ion sources for an electromagnetic isotope separator. Nuclear Instruments 1: 289. 1957.

2. Koch, J. (editor), Dawton, R.H.V.M., Smith, M. L. and Walcher, W. Electromagnetic isotope separators and applications of electromagnetically enriched isotopes. Amsterdam, Netherlands, North-Holland Publishing Co. 1958.

3. Almén, O. and Nielsen, K. O. Systematic investigation of a magnetic ion source for an electromagnetic isotope separator. Nuclear Instruments 1: 302. 1957.

4. Maxfield, F. A. and Benedict, R. R. Theory of gaseous conduction and electronics. New York, N. Y., McGraw-Hill Book Co., Inc. 1941.

5. Penning, F. M. Electrical discharge in gases. New York, N. Y., The MacMillan Co. 1957.

6. Loeb, L. B. Fundamental processes of electrical discharge in gases. New York, N. Y., John Wiley and Sons, Inc. 1947.

7. Present, R. D. Kinetic theory of gases. New York, N. Y., McGraw-Hill Book Co., Inc. 1958.

8. Guthrie, A. and Wakerling, R. K. Vacuum equipment and techniques. New York, N. Y., McGraw-Hill Book Co., Inc. 1949.

9. Slater, J. C. and Frank, N. H. Introduction to theoretical physics. New York, N. Y., McGraw-Hill Book Co., Inc. 1933.

10. Kittel, C. Elementary statistical physics. New York, N. Y., John Wiley and Sons, Inc. c1958.

11. Maitland, A. The influence of pressures within the range 10^{-6} - 10^{-3} mm Hg on breakdown between plane electrodes. Proceedings of the Fifth International Conference on Ionization Phenomena in Gases. 1961. Volume I: 718. 1962.

12. Dushman, S. Scientific foundations of vacuum technique. New York, N. Y., John Wiley and Sons, Inc. 1949.